A study of sub-orbital and millennial-scale climate variability over the past 1.4 million years in the Northern Atlantic.

By
Darrell Ardon Coles

Submitted to the Department of Earth, Atmosphere, and Planetary Science in partial fulfillment of the requirements for the degree of Masters of Science in Geosystems

at the
Massachusetts Institute of Technology
August 1999
[February 2000]

© Massachusetts Institute of Technology. All rights reserved.

Author .....
Department of Earth, Atmospheric, and Planetary Science
August 6, 1999

Certified by .....
Maureen Raymo
Associate Professor of Marine Geology
Thesis Supervisor

Accepted by .....
Ronald Prinn
Department Head

ARCHIVES
MASSACHUSETTS INSTITUTE OF TECHNOLOGY
AUG 2 4 1999
LIBRARIES

Abstract

Spectral methods are used to determine if there are any instances of narrow band oscillations in the climate signal over the past 1.4 million years. The study focuses on the sub-orbital and millennial-scale regime (~1.5 – 20.0 kyr periodicities) at Site 980 and 983, two deep-sea drill sites in the North Atlantic gathered by the Ocean Drilling Program in 1995. The study suggests one such narrow band oscillation in the sediment profile at Site 983, which is discussed from a variety of perspectives.

Other questions addressed include a discussion of potential age-model inadequacies deriving from a potentially 'under-resolved' marine isotope map, as regards high-frequency climate variability. Site 983 has a 4-component sediment profile while Site 980 has a 2-component profile. This paper attempts to resolve the various independent inputs at Site 983 by the method described above. Four proxies have been used in this study; they are magnetic susceptibility, natural gamma, spectral reflectance, and GRAPE (Gamma Ray Attenuation Porosity Evaluator). These proxies are used to inform the millennial-scale issue by coherence methods and are also assessed to see which proxies may prove most useful in future high-frequency research. Finally, a variety of mathematical and statistical methods have been employed including multi-taper analysis with different numbers of Slepian tapers, Singular Spectrum Analysis (SSA), noise background estimation methods (Mann and Lees, 1996), Akaike's Information Criterion for AR(n) model fitting to a data set, and chi-square distribution confidence intervals. These various methods are discussed and evaluated according to their usefulness in sub-orbital research.

Acknowledgements

I would like to personally thank Professor Maureen Raymo for her tireless help in all aspects and phases of this research. I certainly could not have completed even one tenth of this research without all her invaluable advice and ideas. I would also like to thank Professor Carl Wunsch who proved to be a boundless source of information on the mathematical methods employed in this paper. Further, he provided a valuable and critical counterpoint to any and all ideas posed in this paper. It has been a difficult but profound learning experience for me to work under the tutelage of these professors.

Introduction

The climate is a dynamic system that undergoes significant and sometimes surprising variations through time. Although climatology has existed for a long time, the issue of climate change has received an ever-increasing degree of attention in the past decades. This stems both from our ever-improving ability to analyze climatic data via proxy and from the threat of global warming. Climatology faces the formidable task of understanding variations in the climate over time, be they changes in mean global temperature, sea level, global ice cover, oceanic currents, etc. One approach to this topic is to look at the ancient climate to see how it behaved and derive physical principles that might explain this behavior. A vast body of work already exists on this topic but new methods always surface that allow scientists to probe further, with greater accuracy.

High-resolution ocean sediment cores from the North Atlantic are studied in this paper. The cores come from Sites 983 and 980 of Leg 162 of the Ocean Drilling Program conducted in 1995 (Figure 1.0). The data have been analyzed using conventional spectral analysis and SSA (Singular Spectrum Analysis) to derive climate periodicities from the low-frequency Milankovitch cycles to very high-frequency oscillations of only 1 kyr or so. Specifically, we are looking for narrow-frequency-band climate variability, which appears to pervade the records, which extend over a 1.4-myr interval. These variations may signify statistically significant oscillations in the climate signal that, until recently, were nearly impossible to extract from sediment profiles. The sub-Milankovitch oscillations may be Dansgaard-Oeschger type events or Heinrich events, which suggests that the paleoclimate is highly variant on short timescales extending much further back in time than had previously been established (Raymo et al., 1998).

Both sites display multiple-component sediment inputs (Carter and Raymo, 1997). In other words, the sediment at these two sites does not originate from a single source, but multiple, independent sources. Site 980 is thought to be in the simpler setting with two independent inputs, 1) lithic particles from a terrigenous source, and 2) biogenic carbonate (Carter and Raymo, 1997). Site 983 is far more complicated with four components comprising the sediment: 1) terrigenous input via ice rafted detritus (IRD), 2) transported drift muds from Iceland via the Iceland-Scotland Overflow Waters (ISOW), 3) biogenic carbonate, and 4) biogenic silica (Carter and Raymo, 1997). Thus,

derivation of the climate signal depends both upon the facility with which we can isolate these various influences and how we interpret them.

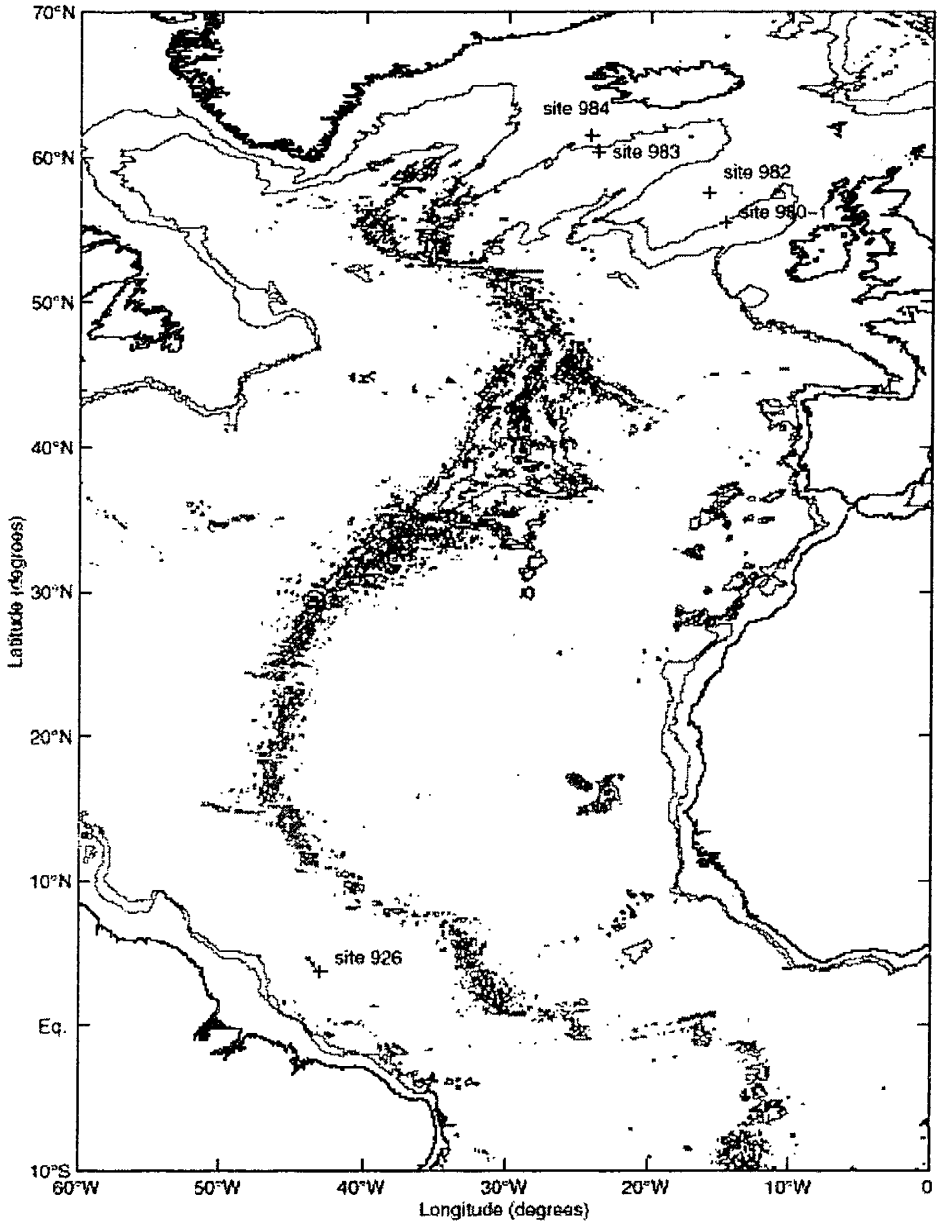

Figure 1.0 Map of the Atlantic region where Sites 980 and 983 are located. Image reproduced from Ortiz et al. (1999).

The analysis was carried out by using a suite of proxies gathered by a multi-sensor track (MST) and split-core analysis track (SCAT) on board the *JOIDES* research vessel. These proxies are magnetic susceptibility, natural gamma, gamma ray attenuation porosity evaluation (GRAPE), and spectral reflectance (a more thorough treatment of

these proxies is offered in the Background Section). These proxies are sensitive to one or more sedimentary inputs (Carter and Raymo, 1997; Ortiz et al., 1999; Jansen and Raymo, 1995) and can generally be categorized by their ability to either record terrestrial or carbonate materials. Carbonates are here assumed to be of pelagic, biogenic origin. Thus, one question addressed is whether complex sedimentation profiles, such as those seen at Site 983, can be teased apart by employing several different proxies in conjunction with each other. A more difficult task is, once we've isolated these various inputs, determining what they tell us about the ancient climate and/or oceanic currents of the North Atlantic.

Site 980 has already been studied by Ortiz et al (1999) and this paper confirms their results and, more importantly, builds upon them. Assuming that there are not substantial intra-regional variations in climate (and that first-order responses to climate forcing are fairly similar between locations) Site 983's proximity to Site 980 makes it an excellent candidate for comparison. This will further inform the questions above.

The proxies used in this study are fairly new to the high-frequency paleoclimate discussion. Magnetic susceptibility and natural gamma measurements have been widely used for studies of climate variability on orbital (Milankovitch) timescales, but they have seen little use at millennial-scale resolution. Spectral reflectance is an altogether new method, which has been employed by Ortiz (1999) with promising results. This paper will assess the robustness of these proxies as indicators of rapid climate variability by comparing the degree of correlation between them.

Lastly, discussion of high-frequency climate variability is impeded by the lack of high-resolution tie points between age and depth profiles (e.g. Ortiz et al., 1999). It is the intent of this paper to discover to what degree uncertainties in time control (chronology) affect our results.

Background

The Ancient Climate Signal

A great deal of research has been performed over the past several decades in an attempt to pinpoint significant oscillations in ancient climate. Several theoretical and empirical observations have been presented, which will be summarized here.

Milankovitch Frequencies

Perhaps the greatest contribution to the paleoclimate field has been put forth by Milankovitch (1930). Milankovitch hypothesized that the climate signal is driven by Earth-Sun orbital variations, which have been theoretically derived. These variations are regional changes in insolation (the amount of incoming sunlight) on Earth's surface. They are governed by three distinct parameters: precession, obliquity, and eccentricity (Crowley and North 1991). Precession refers to the "wobble" of the earth's axis over time (much like a top) and the wobble of Earth's elliptical orbit. Obliquity refers to the angle Earth's rotational axis makes with its orbital plane and eccentricity refers to the out-of-roundness of the earth's orbit. These three parameters vary with periodicities of 100 k.y., 41 k.y., 23 k.y., and 19 k.y. (Crowley and North, 1991). The theory that Earth-Sun orbital variations are the 'pacemaker' of Quaternary climate has been borne out by extensive empirical observation (e.g. Hayes et al, 1976). For example, $\delta^{18}O$ records display strong periodicities at all these frequencies (Hartmann, 1994).

The Milankovitch frequencies have proven invaluable to time-series analysis of the ancient climate signal. The correlation between theory and empirical observations in the oxygen isotope record has led to the creation of the SPECMAP timescale, described below.

Heinrich Events

In his 1987 paper, Hartmut Heinrich described a 7-10 k.y. cycle in the deposition of ice rafted detritus in the North Atlantic. These events were marked by a sudden and large deposition of ice rafted material in sediments, which Heinrich attributed to substantial iceberg calving from glacial sheets (Heinrich, 1987).

The Heinrich events have been considered in the context of $\delta^{18}O$ and percent carbonate (Bond, 1993) records and there is a striking coincidence between these events and other sub-Milankovitch events known as Dansgaard-Oeschger events, which are discussed in the next section. It is suggested that Heinrich events are the result of the 'bundling' together of Dansgaard-Oeschger events until some critical threshold is hit, which causes a massive discharge from the ice sheets. It has been proposed that the Heinrich events are the product of external climatic forcing as opposed to the internal dynamics of glaciers (Bond and Lotti, 1995; Yang et al., 1997). It is speculated that

Heinrich events occur during periods of intense cold when the northern ice sheets are expanding and their shelves can no longer bear the strain of additional ice production (Broecker et al. 1991). Thus, there are significant ice discharge events that deposit ice rafted detritus in significantly higher quantities than the ambient discharge rate. Such variation would obviously be indicative of climate oscillations.

A differing idea is that Heinrich events are caused by internal ice sheet dynamics termed the binge/purge hypothesis (MacAyeal, 1993; Alley and MacAyeal, 1994). This theory proposes that the till (soil, rocks, &c.) found at the base of an ice sheet may be heated geothermally and by friction until a critical threshold is reached. The till then temporarily liquefies and allows the ice sheet to 'purge' into the sea. After a short time, the till re-freezes, the purge phase terminates and the slow buildup of ice recommences. This is known as the binge phase and has been estimated to last between ~6 and ~8 kyr, depending upon initial conditions. Thus, the binge/purge hypothesis does not 'require' climatic forcing as a first-order input. However, climatic forcing would be a second-order input as the rate of ice accumulation is dependent upon climate.

Dansgaard-Oeschger Events

Dansgaard-Oeschger events were originally defined by the high-frequency variability of the climate signal found in ice cores. Their existence is well established back to at least 250 Ka (Dansgaard et al. 1993), and D-O like events have been documented in cores from the early Pleistocene (Raymo et al., 1998). There does not appear to be a single frequency at which these oscillations occur but the characteristic frequencies are between one and several thousand years (e.g. Bond et al., 1997; Oppo et al., 1998)). Originally, these events were studied and derived from the Greenland ice sheet under GISP (the Greenland Ice Sheet Project), and later correlated with paleoclimate data at (e.g.) Vostok, Antarctica (Dansgaard, 1993). In 1993, Bond et al. showed that the Dansgaard-Oeschger events found in the Greenland ice sheet were also present in oceanic sediments. This discovery has led to the extensive use of ocean sediment profiles as proxies for high-variability paleoclimate signals.

Proxies

All but the spectral reflectance measurements were made using the *JOIDES Resolution* Multi Sensor Track (MST). MST data provide high-density samples with a

minimum of effort, coupled with non-invasive techniques so that the samples provide a degree of resolution and accuracy heretofore unapproachable (Carter and Raymo, 1997), (Ortiz et al., 1999). A more detailed explanation of MST can be found in the Explanatory Notes of Leg 162 Initial Reports (Shipboard Scientific Party, 1996). Past research suggest that MST data are very useful as paleoclimate proxies (Carter and Raymo, 1997; Hoppie and Blum, 1994).

Magnetic susceptibility is a measure of the magnetizability of a material. Its application in oceanic sediment analysis pertains to the relative abundance of magnetic materials such as magnetite and iron sulfide found *in situ* in ocean sediments. It has been found that magnetic susceptibility is a good paleoclimate proxy because magnetic materials are not typically oceanogenic (Robinson, 1993). That is to say that magnetic particles found in deep-sea pelagic sediment are not created in the ocean but are usually transported there by some physical process. One such physical process is ice rafting. Ice rafting refers to the transport of terrigenous materials by ice. Ice rafted detritus (IRD), as it is called, is transported by icebergs that have calved from continental ice sheets, including (e.g.) the Greenland ice sheet and Antarctic. As these icebergs encounter warmer seas and air, they begin to melt and they deposit the terrigenous material scraped from the land surface, which includes magnetic particles such as those mentioned above. Therefore, in some regions magnetic susceptibility measurements can provide an indirect proxy for regional ice volume, under the assumption that iceberg calving is a function of ice sheet size (Ruddiman, 1987). Since $\delta^{18}O$ and magnetic susceptibility are proxies for ice volume in the North Atlantic, magnetic susceptibility should display the Milankovitch periods. Furthermore, we would expect to see a strong first-order response to ice rafted material deposited during characteristic Heinrich events.

Aside from the ice rafted input of magnetic materials, magnetic susceptibility has also been found to detect terrigenous materials delivered by ocean currents and ash falls in the North Atlantic (Carter and Raymo, 1997; (Robinson, 1993). This is particularly important at Site 983, which is thought to be a two-component system with regards to magnetic susceptibility. The two components are the influx of terrigenous material from the surface via IRD, and the transport of fine drift muds, rich in magnetic materials, by bottom currents. These currents are the ISOW (Iceland-Scotland Overflow Waters),

(Carter and Raymo, 1997) whose strength may be an indicator of the intensity of deep-water production in the region, a facet that affects climate change. This complicates the interpretation of magnetic susceptibility at this site because MS responds both to IRD events as well as the strength of the oceanic current that transports terrigenous materials.

To further complicate matters at Site 983, there are believed to be at least two other independent components that comprise the sediment: biogenic carbonate and biogenic silica (Carter and Raymo, 1997). Although these inputs do not affect magnetic susceptibility (Robinson, 1993), they do complicate the sedimentary stratigraphy. However, it may actually be beneficial if other proxies are introduced that are known to be sensitive to specific inputs. Thus, it may be possible to 'tease' apart the various components of the magnetic susceptibility (e.g.) into their climatic influences and their sediment transport influences. Another approach may be to examine and compare similar proxies at a location that displays simpler sedimentary properties. Site 980, located on the east side of the Rockall Plateau is a good candidate. While Site 983 is a four-component system, Site 980 is only a two component system (Carter and Raymo, 1997).

A second proxy, natural gamma, is a measure of the emission of gamma rays, as radioactive particles decay. Radioisotopes with sufficiently long half-lives are usually studied. These particles include ^{40}K (potassium), ^{232}Th (thorium), and ^{238}U (uranium), all of which can be found in clays, shales, phosphates, sandstones, arkosic silts, etc (Hoppie, Blum et al., 1994). Preliminary research on MST data proxies has concluded that natural gamma is very responsive to terrigenous input such as felsic IRD and lithic particles (Carter and Raymo, 1997). Since magnetic susceptibility indicates ice volume according to the input of terrigenous material, we would also expect to see a similar signature in the natural gamma signal. Thus natural gamma at Site 983 may be very helpful in separating the ice rafted component from the sediment transport component because the fine material transported by the ISOW is primarily basaltic in origin and therefore characterized by low natural gamma radiation (Carter and Raymo, 1997).

A third proxy, gamma-ray attenuation porosity evaluator (GRAPE), is used to measure the wet-bulk density of sediment. Wet-bulk density refers the density of a core sample as a function of the sum of its dry mass and water mass divided by the sum of its dry volume and water volume (with necessary corrections due to salinity):

$$\rho_b = (M_s + M_{pw})/(V_s + V_{pw})$$

In effect, it is a proxy for estimating the mass accumulation of pelagic sediments and for calculating the porosity and void ratios of those sediments (Shipboard Scientific Party, 1996). GRAPE achieves an estimate of the bulk-wet density by measuring the electron density of a sample, which is logarithmically related to the gamma-ray attenuation (Shipboard Scientific Party, 1996). A more detailed discussion of GRAPE can be found in the Explanatory Notes of the Leg 162 Initial Reports (Shipboard Scientific Party, 1996; Boyce et al., 1976).

Theoretically, there is a characteristic density to the carbonate material found in pelagic sediments. GRAPE can then be thought of as a variable ratio of the carbonate content to other inputs such as ice rafted material, which will have a different characteristic density/mass. Thus, GRAPE should indirectly record the dilution of carbonate with respect to terrigenous input. This may prove useful in deriving the relative influence of biogenic and physical transport inputs at sites displaying multiple-input sedimentation profiles.

The fourth proxy, spectral reflectance, is the only proxy considered in this paper that was not initially recorded by the MST on board the *JOIDES Resolution*, the Ocean Drilling Program vessel. Spectral reflectance data are measured by an instrument called split-core analysis track (SCAT), which gathers and stores discrete light spectrum measurements over the length of the core. For a more detailed explanation of the methodology, the reader is referred to Ortiz et al. (1999) and the Shipboard Scientific Party (1995). Spectral reflectance is a proxy for percent carbonate (Ortiz et al., 1999), (Shipboard Scientific Party, 1995). The color of a core interior can be analyzed to derive its sedimentary composition according to the spectrum of the light it reflects, ergo, spectral reflectance works as a percent carbonate proxy. As previously mentioned, reflectance has already been analyzed at Site 980 for frequencies from secular to ~1/5000 kyr. However, it may also prove fruitful in trying to infer the influence of sediment transport by oceanic currents, which will further aid in interpreting the spectra at Sites 980 and 983.

Figures B.1 and B.2 show the plots of the four proxies at Sites 980 and 983.

Given this basic understanding of the four proxies studied in this paper, spectral analysis may be carried out to determine statistically significant periods that may arise in these data sets. Coherence tests may be applied in an attempt to isolate the paleoclimate signal from signals derived from other influences such as those mentioned above.

Brief Note on Sediment Retrieval, Data and Analysis

The choice for a drill site must be carefully deliberated considering the estimated rate of deposition of sediment. A location that has too low a sedimentation rate will be extremely difficult to analyze with regard to high-frequency oscillations. Sites 983 and 980 were chosen in consideration of this fact, and were gathered from the Bjorn (61°N 23°W) and Feni (60°N 14°W) Drifts, respectively. Deep-sea currents that erode sea sediment in one location and deposit them in another created these drifts (Jansen and Raymo, 1996). The sedimentation rates in these regions are thought to be in excess of 10cm/kyr, which allows high-resolution sediment profiles to be constructed. The sampling intervals at both sites, after age-models had been fit, averaged from $\Delta t \cong 200$ to $\Delta t \cong 1000$ years (magnetic susceptibility and GRAPE; natural gamma and spectral reflectance, respectively). Periodic frequencies thus can be studied from ~1/400 years to ~1/2000 years (the Nyquist frequency) for these proxies.

$\delta^{18}O$ records have provided the backbone for paleoclimatic studies and have been used to create a standard chronology known as the SPECMAP timescale (Imbrie et al., 1984). Raymo (1997) described the SPECMAP approach as follows:

> The SPECMAP timescale, developed by tuning to [Milankovitch frequencies], provided a chronology to which almost all paleoclimate records could be tied via their correlative and characteristic $\delta^{18}O$ record. This timescale has been the cornerstone of Quaternary paleoclimate studies for over 10 years.

The SPECMAP timescale has revolutionized paleoclimate studies of pelagic sediments but it may still have distinct limitations. To create an age-model, correlations are derived between the proxy signal (typically $\delta^{18}O$) and the standardized marine isotope chronology (Shackleton, Berger, and Peltier, 1990). These correlations are 'tied' or interpolated onto the new record, creating the age-depth model. One problem that occurs when paleoclimate signals are analyzed in the frequency domain is that the isotopic map

does not have millennial-scale resolution. Any data interpolated between tie-points is done so linearly. Thus, if the sedimentation rate *between* tie-points is highly variable, the interpolated data in that regime will not accurately reflect the true age of the strata. This will affect the spectral analysis, causing erroneous peaks to arise and generally masking any significant peaks that may exist.

All else being equal, there are a variety of methods for performing the actual time-series analysis. The standard method is Fourier analysis, which has many variations for these purposes. Another method is singular spectrum analysis, a newer method based upon eigenvectors/values of the lagged-covariance matrix of the data set (Cortijo, 1995; Elsner and Tsonis, 1996). Once efficient statistical methods have been established for singular spectrum analysis, it may prove invaluable as a spectral analysis tool (this method is used to filter several of the data sets studied in this paper). The data analyzed at Site 983 spanned approximately 1.4 myr and Maureen Raymo provided the age-model.

The data at Site 980 was also analyzed over 1.4 myr and both Joseph Ortiz and Maureen Raymo provided the age-model. Reflectance at Site 980 has already been discussed for periodicities from 100 kyr to ~5 kyr (Ortiz et al., 1999). This study verifies their results and also focus on shorter periodicities, ranging down to the Nyquist frequency (~1/2000 years). Ortiz has stated that the sampling interval and the accuracy of the age-model at this site do not allow accurate results at high frequencies. The veracity of this claim will be tested by comparison with other proxies both at Site 980 and 983.

Methods

Analysis

Spectral analysis is a means by which periodicities within a time series may be quantified and studied. The data were analyzed in two or three ensembles, each ranging over an interval of 500 kyr except for the third ensemble (where applicable), which was analyzed over a 400 kyr interval. Three proxies were analyzed at Site 983: magnetic

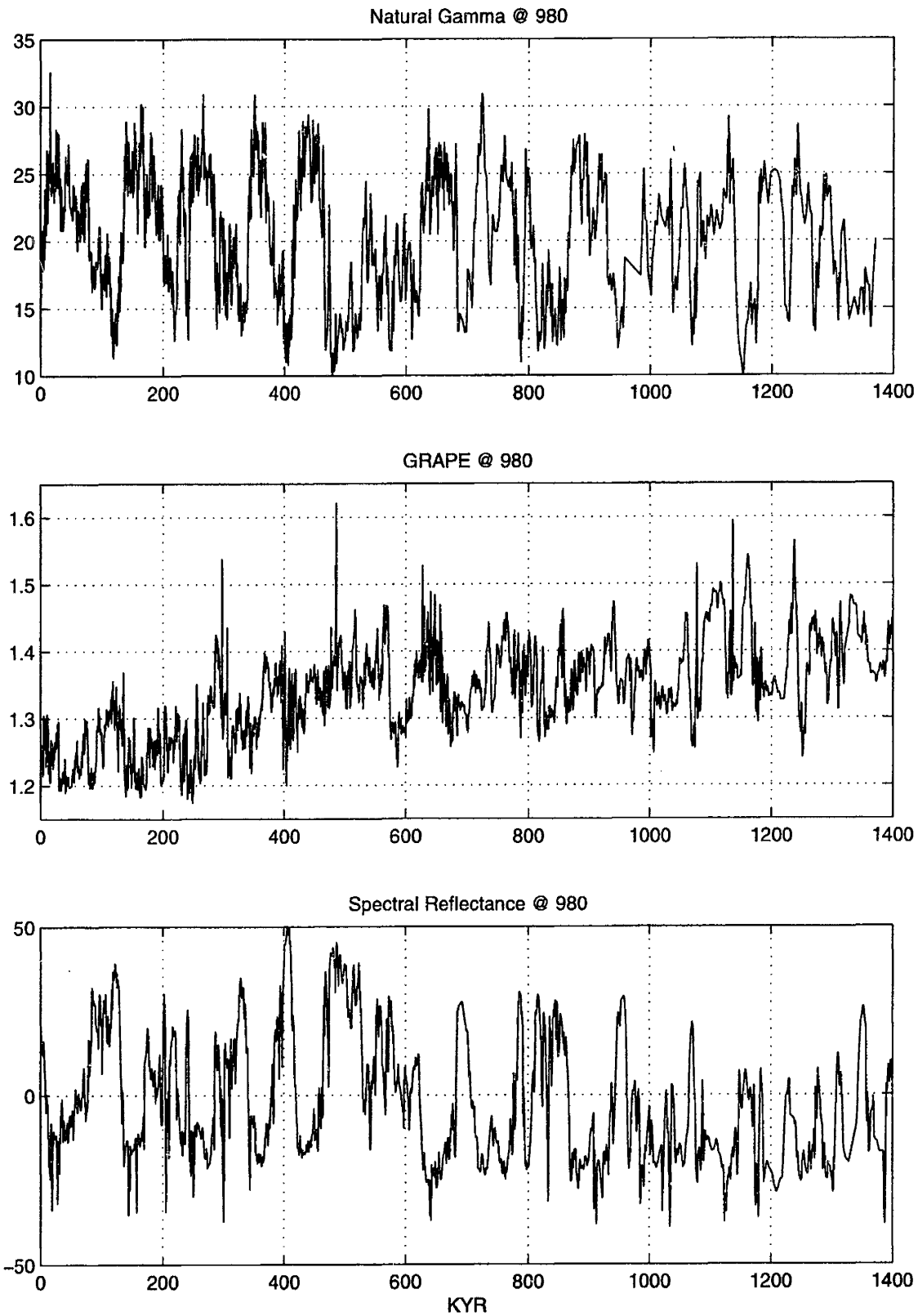

Figure B.1 Plots of Spectral Reflectance, GRAPE, and Natural Gamma at Site 980 over the past 1.4 myr.

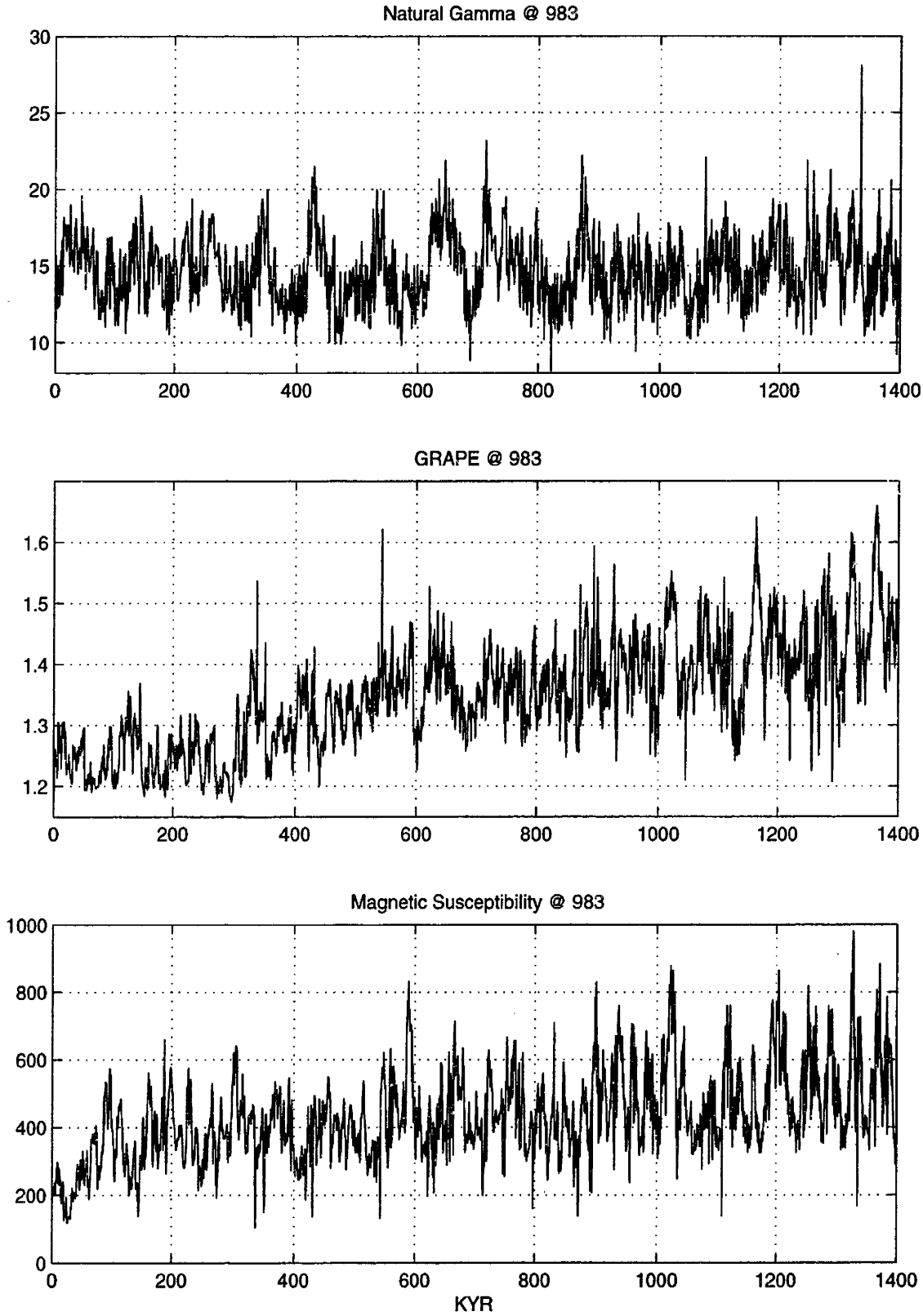

Figure B.2 Plots of Magnetic Susceptibility, GRAPE, and Natural Gamma at Site 983 over the past 1.4 myr.

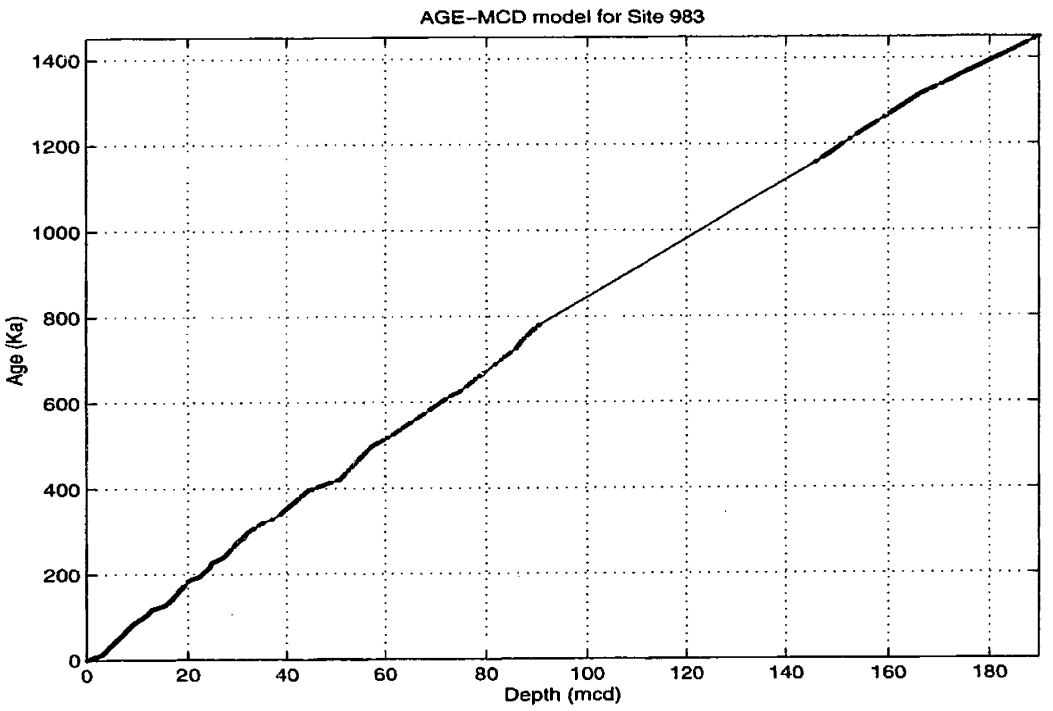

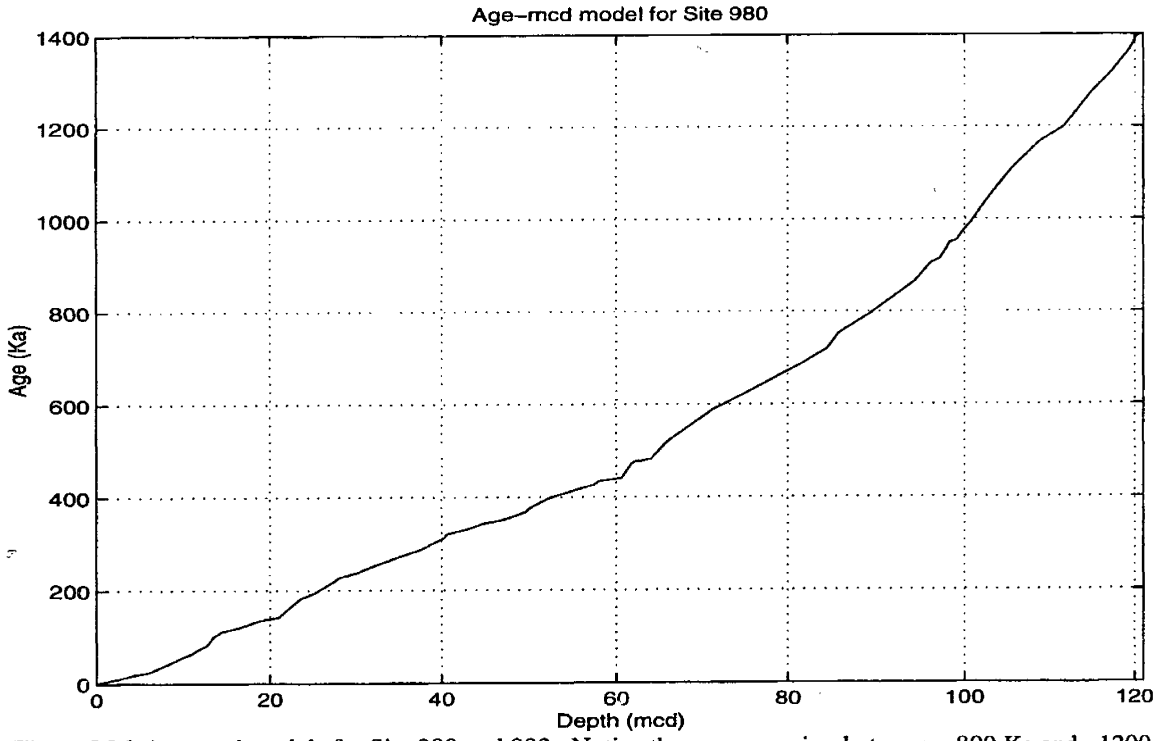

Figure M.1 Age-mcd models for Site 980 and 983. Notice the gap occurring between ~800 Ka and ~1200 Ka at Site 983. This interval was simply linearly fit as the thin line suggests.

susceptibility, natural gamma, and GRAPE. Three proxies were also considered at Site 980: reflectance, natural gamma, and GRAPE.

The analyses performed in this paper make the *a priori* assumption that these time series are essentially stationary. That is to say, the statistics that 'govern' these data sets are time-invariant. Evidence suggests that the climate signal is, in fact, not entirely stationary but displays appreciable statistical variation at the time boundary of ~950 Ka (Ortiz et al., 1999). Therefore, the ensembles have been broken at the ~1 Ma in an attempt to account for this fact. It does not appear that the 50-kyr overlap has had an appreciable effect upon the analyses within this interval.

A modified version of classical Fourier Analysis was used to analyze the data. Thomson's Multi-taper Method was utilized with 3 to 7 Slepian tapers and eigenvalue weighting of the average was employed, similar to the method described by Mann and Lees (1996). A more thorough explanation of the mathematics is given in the appendix. The greatest concern when performing spectral analysis in the search for paleoclimatic signals is the estimation of the noise background against which we are trying to extract these signals. Mann and Lees have suggested a robust red-noise background estimation scheme (1996) whereby we more accurately deduce the background noise. This method is broken into several sub-procedures, which have been employed in a modified form. The basic procedure goes as follows: 1) Perform a multi-taper estimate of the original data, 2) perform an F-test for periodic signals based on the ratio of the variance of a pure sinusoid at a given frequency to that explained by the spectral estimate at that frequency, 3) Reshape those areas of the spectrum that pass the F-test so that they no longer appear 'significant', 4) Median smooth the reshaped spectrum to get a better overall estimate of the noise structure, and 5) Create an estimate of the noise structure with a simple autoregressive model (Mann and Lees, 1996). A more detailed discussion of the mathematics is given in the appendix.

As previously stated, the spectral estimate was made using the MTM with 3 to 7 tapers. The F-test utilized was slightly modified from that used by Mann and Lees. An iterative Matlab routine was created, which performed the F-test but weighted the values of the F-test such that the routine was more likely to reshape lower frequency signals.

The motivation behind this is that the majority of useful information we derive from Fourier analysis of paleoclimatic signals occurs at frequencies ranging from 100 kyr to 1

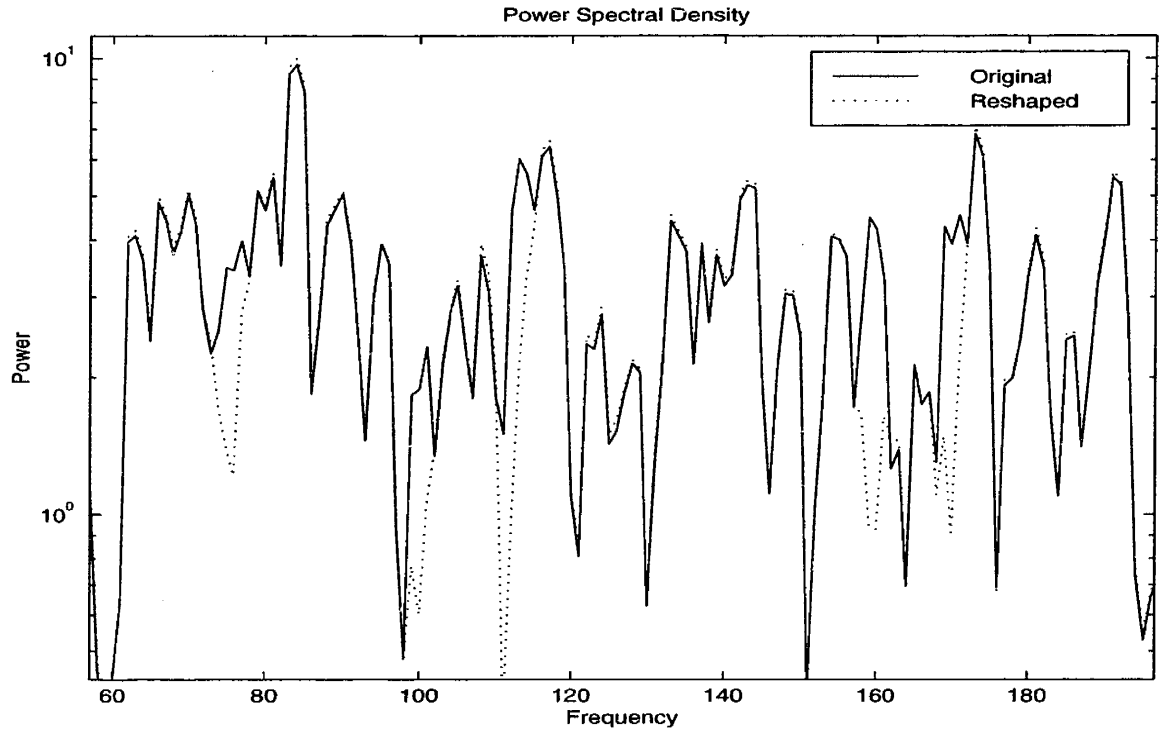

Figure M.2. Example of the original and reshaped spectrum of a white-noise process. The hashed line depicts the reshaped spectrum.

or 2 kyr. However, the original spectrum will contain a great deal of information at higher frequencies that do not interest us or that we cannot reasonably resolve. Since we are going to ignore the very high-frequency signal in the spectrum, there is no need for us to consider it when we are making our estimation of the background noise. Thus, a simple linear weighting vector was introduced to the F-test starting with a multiplier of 7 at the lowest frequency and decreasing linearly to a value of 1 at the highest frequency. Although this may seem somewhat unorthodox, the results bear out the utility of this method.

Clearly, the number of Slepian tapers we use in our power density spectral estimate will bear upon the resolution we can achieve in the frequency domain. The greater the number of tapers we employ in making the spectral estimation (typically from 8 to 16 tapers), the greater the frequency bandwidth we are averaging. This smooths the power density spectrum, which permits us to assess the overall spectrum better. Conversely, using only a few Slepian tapers (from 3 to 5) allows for greater resolution in

the frequency domain since we are generating a more 'localized' average of spectral power. A tradeoff arises between frequency resolution (in the narrow band and/or line frequency sense) and overall spectral shape (in the broad band frequency sense). While narrow band or line spectra allow us to pinpoint particular frequencies 'better', there is a considerable risk in asserting that these frequencies are in fact 'real' oscillations in the climate record. In effect, the use of only a few Slepian tapers in spectral estimation implicitly assumes that oscillations we find to be significant must essentially be purely (or nearly) sinusoidal, or of the form:

$$a\cos(t\pi/T)+b\sin(t\pi/T)$$

Where a and b are constants, $2T$ is the period of the oscillation, and t is time (which is defined as $t = n\Delta t$, where Δt is the sampling rate and n is the sample number). Obviously, we would not expect to see pure sine waves in many places in Nature. However, this study attempts to assess the frequency domain of these proxies by using narrow band and line spectra. Should any instance arise where such narrow band frequencies agree across proxies and sites, it would provide strong evidence that the climate or a climate-forced mechanism is oscillating in a nearly sinusoidal manner through time. This would be a very remarkable discovery.

The reshaped signal thus represents our estimate of the noise background spectrum, where we have 'taken out' all those frequencies that *may be* significant according to the F-test. The approach used to reduce the spectrum at these frequencies was as spare as possible. The idea was simply to reduce the power at a given frequency (that had passed the F-test at the 99.99% level) to that of the surrounding spectrum. Somewhat arbitrarily, the mean value of the target spectrum, to which this frequency would be adjusted, was derived from a 14-point spread on either side of the frequency and the 'adjusted' frequency would include its two neighboring points. The typical frequency bandwidth for averaging the spectrum was ~0.04 (where the frequency is in cycles/kyr). Bear in mind that the averaging window then is a function of the targeted frequency since a target frequency of 100 kyr would be adjusted to the average power of the spectrum over a ~25 kyr bandwidth, for example. The result is a minimally 'invasive' reshaping of the original spectrum (Figure M.2.). Thus, reshaping amounts to

the removal or reduction of power at specific frequencies in an attempt to better estimate the background noise.

Once the spectrum has been reshaped, a median smoothing is performed with a typical window of ~30 points. This has the effect of making a better overall estimate of the noise background (Ortiz et al., 1999; Mann and Lees, 1996). However, one of the problems inherent in reshaping a spectral signal is a loss of variance in the new signal. If one is not careful, the estimate of the ambient noise background by this method will result in a noise spectrum that has far too little energy, the result of which is the discovery that much of the original spectrum appears to be statistically significant. It was found that a simple adjustment could be performed, to account for this variance loss.

$$m = +\sqrt{\frac{\overline{F}_X}{\overline{F}_N}}$$

$$\overline{F}_X = E[|F(X(t))|^2]$$

$$\overline{F}_N = E[|F(N(t))|^2]$$

where $F(X(t))$ and $F(N(t))$ are the Fourier transforms of $X(t)$ and $N(t)$ such that $X(t)$ is the original data set and $N(t)$ is the reshaped data set, which has undergone some variance loss. Then, introducing the notation

$$S(X(t)) \cong S(mN(t))$$

where S is the power spectral density function (and therefore actually a function of *period* or *frequency*; a short proof is given in the appendix). Thus, we are stipulating that the total energy of the estimated background noise should be very close to that of the original data. From a statistical point of view, this is desirable if we are to make reasonable hypotheses about frequencies that are potentially significant. This method may overestimate the background noise somewhat but, again, the results of this study tend to lend credence to it (Figure M.3.).

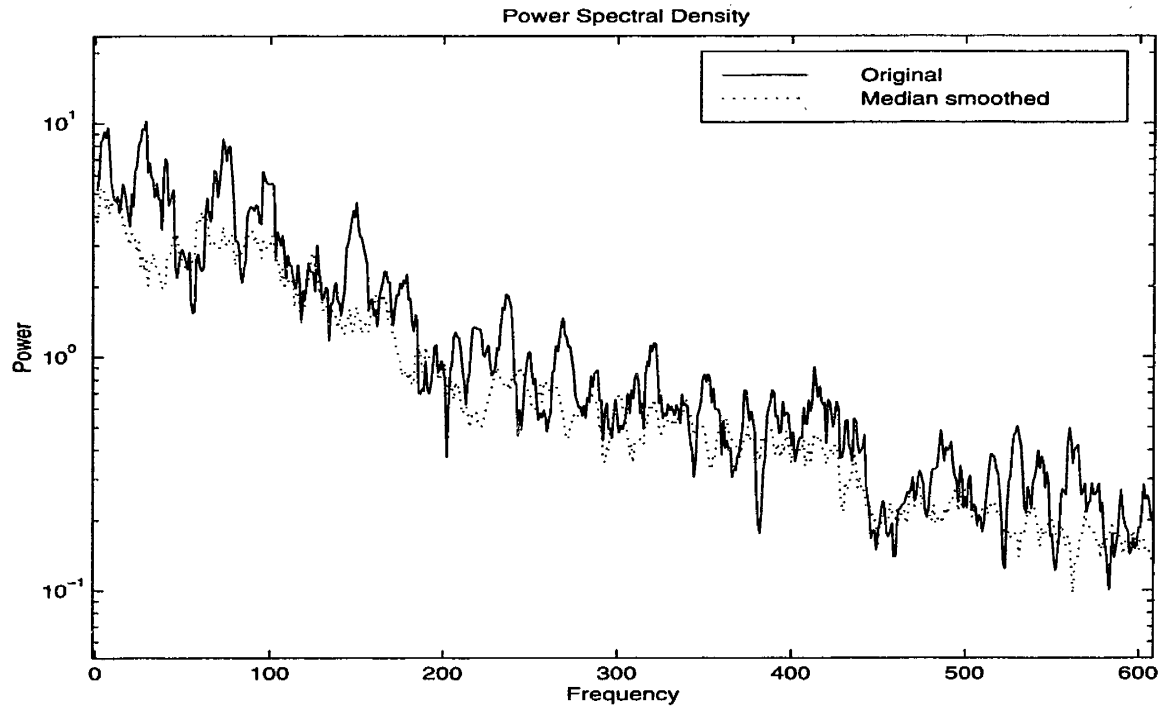

Figure M.3. Spectral density functions of an AR(1) Process and its reshaped, median-smoothed, variance-adjusted noise estimate.

Once an acceptable estimate of the background noise has been made from the sample data, we must derive confidence intervals. Although it has been suggested that the best estimate of the noise structure should be an AR(1) process (Mann and Lees, 1996), this guideline is ignored. For the sake of argument, suppose we know that the climate is strongly correlated over a ~1000 year interval. If our sampling rate were 1000 years, then an AR(1) model would suffice to capture the assumed autocorrelation present in the climate signal (the autocorrelation of an AR process typically decays away exponentially, which is in agreement with our intuition about the oceanic forcing of the climate on millennial scales). However, the sampling rates for Sites 983 and 980 were between ~200 and 1000 years for different proxies; GRAPE and magnetic susceptibility were both densely sampled while reflectance and natural gamma were sampled at $\Delta t \cong 1$ kyr. Thus for densely sampled proxies, an AR(1) process would not sufficiently explain the autocorrelation we would expect to find in the paleoclimate signal. An AR(4) or AR(5) process would be well suited for complying with the assumption that the climate signal must be autocorrelated on a time scale of ~1000 years. The disadvantage of using higher order AR models is that we may introduce periodicities into the estimation of the

noise structure that 'mask' significant frequencies in the original data (Mann and Lees, 1996; Priestley, 1996). The worst that could happen is that we may overlook a weak signal that is significant. On the other hand, a slightly overestimated noise background gives us an added advantage in determining statistical significance. Therefore, the decision was made to err on the side of safety with a (perhaps) slightly overestimated noise background.

To test this hypothesis, Akaike's Information Criterion (see appendix) was carried out on all records. The finding was that, given a good estimate of the median- smoothed red noise background, the information criterion always suggested an AR(4) or AR(5) process for densely sampled proxies and an AR(1) or AR(2) process for the less densely sampled ones. The Yule-Walker method (the default method in Matlab) was used to determine the parameters of the AR processes in each instance. Thus, AIC and other hypothesis tests might be very useful in estimating the characteristic autocorrelation of ancient climate, which may assist in understanding the underlying physical mechanisms driving these complex systems. The Monte Carlo method was used to create 10000 surrogate records for use in determining confidence levels.

In some cases, it was found that the concentration of power at low frequencies caused the background noise estimation to be biased toward these frequencies. In such cases, where a reasonable estimation of only the higher frequency noise was required, filtering by SSA (Singular Spectrum Analysis) was utilized. The window length was taken to be ¼ the length of the entire record and typically the first 5 to 10 eigenvalue pairs were withheld when reconstructing the filtered time series. A thorough treatment of this subject may be found in Elsner and Tsonis (1996) or in Cortijo (1995). The method is also briefly described in the appendix.

It is also important to point out that aliasing is a serious concern in discrete time series analysis. The greatest resolution we can achieve with these proxies in the frequency domain is ~400 years (the Nyquist frequency for GRAPE). Presently, we do not know what the continuum may look like beyond this point. If there were a very high-frequency component to these time-series that simply could not be resolved, the effect of undersampling (relative to this frequency) would be to alias this frequency. This would manifest itself as some concentration of power at some lower frequency (dependent upon

the sampling rate and the 'true' frequency). This fact cannot yet be rigorously addressed, as the sampling rate simply does not permit this degree of resolution. There may also be very large errors in the spectral estimate at such high frequencies, due to potential age-model inadequacies.

All spectral density plots in this paper display the estimated power spectrum, the estimated red-noise background (the hashed line), and the 90%, 95%, and 99% confidence levels. The spectral analysis of the proxy data was broken into a log-log plot typically covering the 0 – 0.25 frequency band. This corresponds to frequencies ranging from secular to ~1/4000 years. This allows a closer inspection of frequencies in this band. Corresponding log-linear plots were generated for the frequency band from 0.18 to a maximum of 0.75 (depending upon the sampling frequency of the data), which covers frequencies from ~1/5600 years to ~1/1300 years. All spectral plots are arranged so that the y-axes (spectral power axes) display a similar range of magnitude on the log scale. This allows us to visually inspect the spectral estimates to see if they display similar shapes. The x-axes (frequency axes) cover the same range of frequencies as well.

Although the Nyquist frequency of some samples would allow for resolution down to ~1/400 year, the spectral analysis at such high frequencies would be very sensitive to the accuracy of the age-depth model (discussed in the Background section). It was decided that the scale age-depth model would compromise the resolution of such high-frequency information. Therefore, no frequencies higher than 1/1300 years are considered in this paper.

In this paper, reference is made to Heinrich-type or D-O type events, which is only used as a guide for the reader to identify which frequency regime is being discussed. Unless otherwise specified, the use of these terms does not necessarily imply that spectral peaks in these regimes are due to climatic inputs.

Results

Site 980

Ortiz et al. (1999) have already considered spectral reflectance at Site 980 from secular trends to periodicities of ~5000 years. To verify the analytic methods utilized in this paper, their results are compared with my own (Figure 2.0). The spectral densities agree almost completely over all significant values that Ortiz derived. Furthermore, the narrow-frequency-band method used in this paper also indicates the 19 kyr periodicity. Therefore, the method used in this paper appears to be quite robust.

It is informative to make a comparison between spectral estimations made with few Slepian tapers and those made with several. Figure 2.0.c displays the spectral estimate, made with 8 Slepian tapers, of reflectance at Site 980 over the 950-kyr interval. Observe that figure 2.0.b, made with 4 Slepian tapers, is much more 'jagged' than 2.0.c. Furthermore, the ~19 kyr and 6.5 kyr line frequencies are absent from Figure 2.0.c. This illustrates the fact that a more smoothed spectral estimate can behave very similarly to a less smoothed one, but there may be appreciable differences as well. The use of the chi-square 95% confidence interval then provides an excellent crosscheck to assess potentially significant line frequencies in these spectral estimations. Thus, the use of the standard chi-square confidence interval informs the search for significant narrow band and line frequencies in the climate record as well as the degree to which we may believe significance according to the noise background estimation (NBE) method.

Having established the viability of the analytic methods used here, we may now consider millennial-scale trends that appear in the three proxies at Site 980. Recall that Site 980 is a two-component sediment system. Thus, analysis at Site 980 should inform the analysis at Site 983.

The incidence of statistically significant peaks at sub-orbital frequencies is difficult to characterize. The nature of the analysis employed allows for such a high degree of resolution within the frequency domain that it becomes difficult to specify which frequency actually best signifies a 'true' peak. When this case arises, a visual estimate of the median frequency (typically) is inferred from the overall spectral shape of the frequency regime in question. GRAPE displays a pacing of ~12.5 to 13.5 kyr over

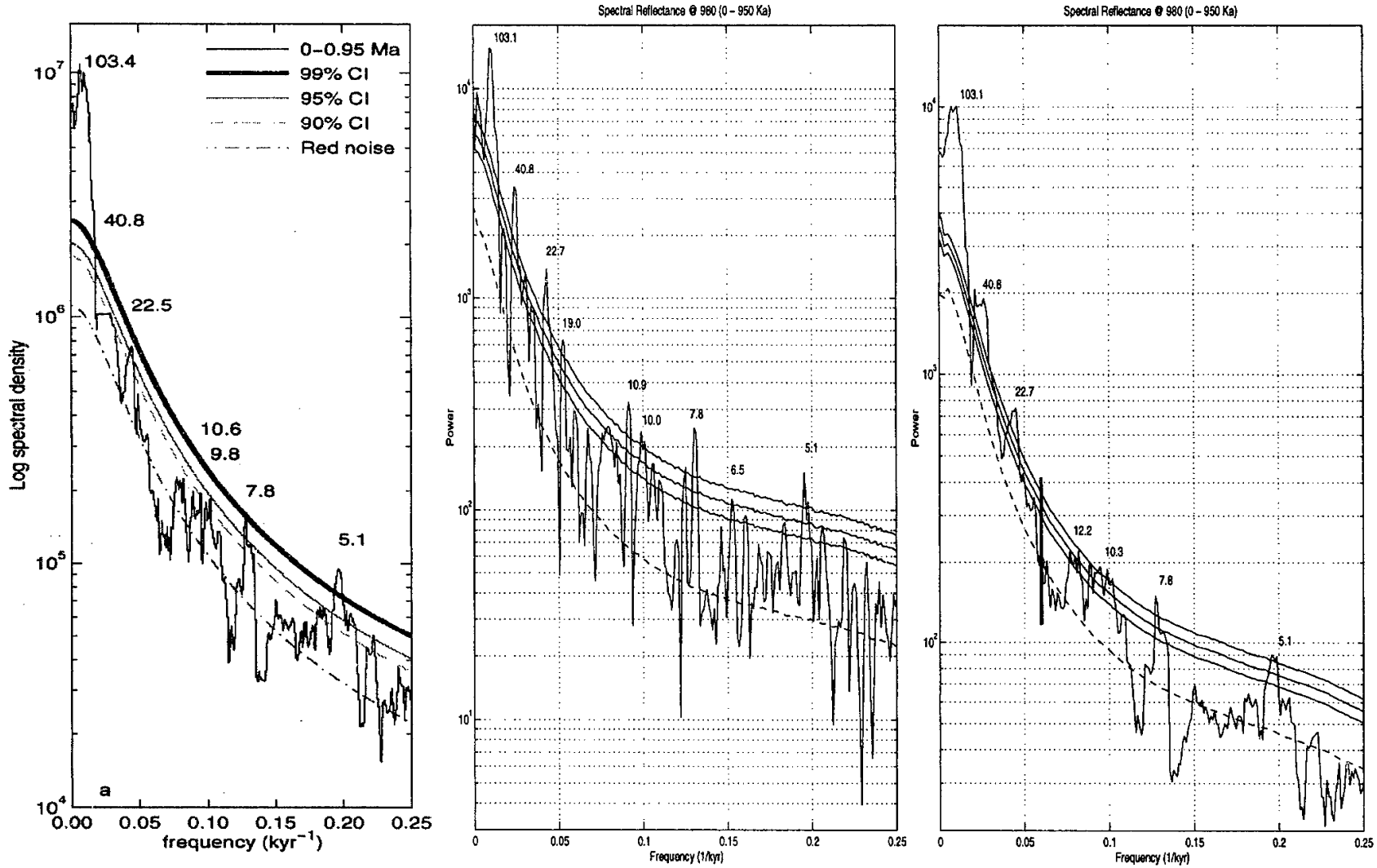

Figure 2.0 Spectral density plot of reflectance data at Site 980 over 950 kyr. (a) is reproduced from Ortiz et al. (1999). In all plots, the dashed line represents the background noise estimation and the three lines above indicate the 90%, 95%, and 99% confidence intervals. Note the close agreement between all figures displayed by the two methods. Figure 2.0.c is the spectral estimation with 8 Slepian tapers instead of 3 (in Figure 2.0.b). Also notice the χ^2 confidence bar in (c), which is the dark line with an 'o' centering it on the mean background.

the 1.0 Ma interval (Figures 2.1.b and 2.3b) while spectral reflectance displays significant frequencies within this regime over the 0.5 – 1.4 Ma interval (Figure 2.3.a and 2.5.a). Natural gamma displays a potentially significant concentration of power over this frequency regime (Figures 2.1.c, 2.3.c, 2.5.c), relative to the χ^2 95% confidence level. GRAPE displays significant periodicities at ~9.3 - 9.5 kyr over the 1.0 Ma interval (Figure 2.1.b and 2.3.b) and reflectance indicates a ~10.1 kyr oscillation over the 0.5 – 1.4 Ma interval (Figure 2.3.a and 2.5.a). It is not clear whether this periodicity may indicate the same physical process or whether GRAPE and spectral reflectance are responding to entirely different signals. The dissimilarity between these two proxies in the frequency and age domains suggests that they are either responding to independent forcing or that there are significant age model discrepancies. Imposing bandpass filters and comparing these signals in the time domain might elucidate this question. Coherence plots between all three proxies (Figure 2.7 – 2.9) within this regime show no consistent correlation. In the broad band sense, the GRAPE coherence plots do suggest some degree of correlation over the ~8.8 – 11.0 kyr interval. However, there is no compelling evidence for narrow band coherence between these proxies within this frequency band.

Ortiz et al. (1999) have suggested that this regime may actually be due to harmonic combinations of the Milankovitch frequencies. Indeed, a combination of the precession and obliquity cycles would produce 1/19 + 1/41 = 1/12.98 kyr or 1/19 + 1/23 – 1/41 = 1/13.94 kyr (Ortiz et al., 1999). It is not known how viable this hypothesis may be, however it does provide a compelling argument for the incidence of potentially significant spectra within this frequency band.

Spectral reflectance also shows a ~7.7 – 7.9 kyr concentration of variance (Figure 2.1.a and 2.3.a) over the past 1 myr. This periodicity is unique to the spectral reflectance signal with the exception of peaks at 7.2 and 8.2 kyr in the GRAPE spectrum over the 1.0 –1.4 Ma interval (Figure 2.5.c). The coherence plots show absolutely no correlation between proxies over the entire age interval at these frequencies. Thus, in the narrow band sense, there appear to be no significant peaks between 7.2 – 8.2 kyr. Again, the degree of coherence suggests correlation between GRAPE and the other two proxies from ~8.8 – 11.0 kyr. This appears to be the only potential significant frequency band within the Heinrich regime.

Although not significant at a 99% level (Figure 2.1(a) – 2.6(a)) according to the noise background estimation, there appears to be a consistent peak centered at ~5 kyr within the spectral reflectance data, which is in accord with the findings of Ortiz et al. (1999). The GRAPE data also seem to display a periodicity roughly within this regime (Figure 2.2.b and 2.4.b). However, this frequency regime within the GRAPE spectra does not display as consistent a narrow band spectrum as the reflectance data. The shape of the GRAPE spectrum at ~1/5000 kyr is much broader over the 0 – 500 Ka interval, while the spike in the 500 – 1000 Ka interval displays an appreciable transient. Coherence tests between GRAPE and reflectance show no correlation centered at the ~1/5000 year frequency. Furthermore, the natural gamma signal shows an apparent lack of power or consistence at this periodicity. Coherence tests between natural gamma and the other two proxies display no compelling correlation (Figure 2.7 and 2.8) either in the narrow band or broad band sense. Therefore, if a statistically significant amount of variance is truly displayed in the reflectance signal, it appears to be more broad band (from ~4.8 – 6.0 kyr) and it is unique to the reflectance proxy. In this instance, the χ^2 confidence interval appears to confirm the findings via the noise background estimation method.

There also appears to be a concentration of variance within the 2.5 – 2.7 kyr period band reflected both in the GRAPE signal and spectral reflectance (Figure 2.2(a,b), 2.4(a,b), 2.6.b). The coherence plots between reflectance and GRAPE (Figure 2.9) suggest no correlation within this period band. This again suggests that there is no real line frequency present at exactly these frequencies within pelagic sediment profiles. There is no statistically significant peak found in the natural gamma data at these frequencies (Figure 2.2.c, 2.4.c, and 2.6.c) either. However, coherence tests between natural gamma and the other two proxies (Figure 2.8 and 2.9) do display a potentially significant correlation at periodicities of ~2.2 – 3.3 kyr over the past 1.0 myr. Much heavier smoothing of the spectra and coherences is necessary to test this result. Thus, while there is some potentially significant concentration of variance at a period of ~2.0 to 3.0 kyr, there is no evidence suggesting a clear cut line frequency that is persistent in all proxies. The spectral estimations do suggest a near proxy-wide agreement at ~3.1 – 3.4 kyr periodicities. This periodicity is found throughout the natural gamma and GRAPE

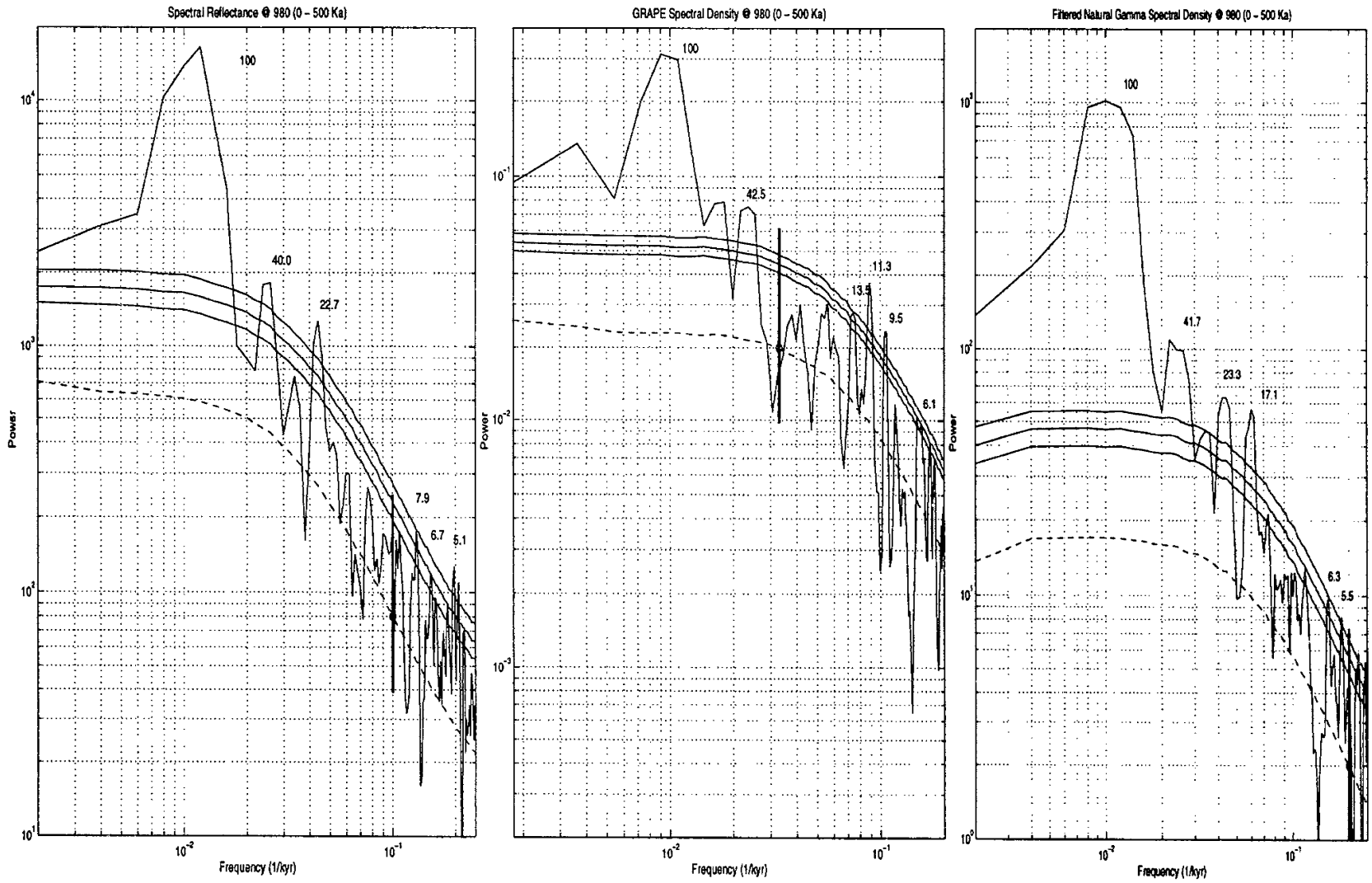

Figure 2.1 Spectral reflectance (a), GRAPE (b), and Natural Gamma (c) spectral density plots over the 0 to 500 Ka interval at Site 980. The hashed line represents the estimated median red-noise background and the three lines above the noise estimate are the 90%, 95%, and 99% confidence intervals. Note: Log-log plots have been used to generate these spectral estimates over this frequency band (secular to ~1/4000 years). Corresponding log-linear plots can be found on the following page, for the frequency band from ~1/5000 years to ~1/1300 years.

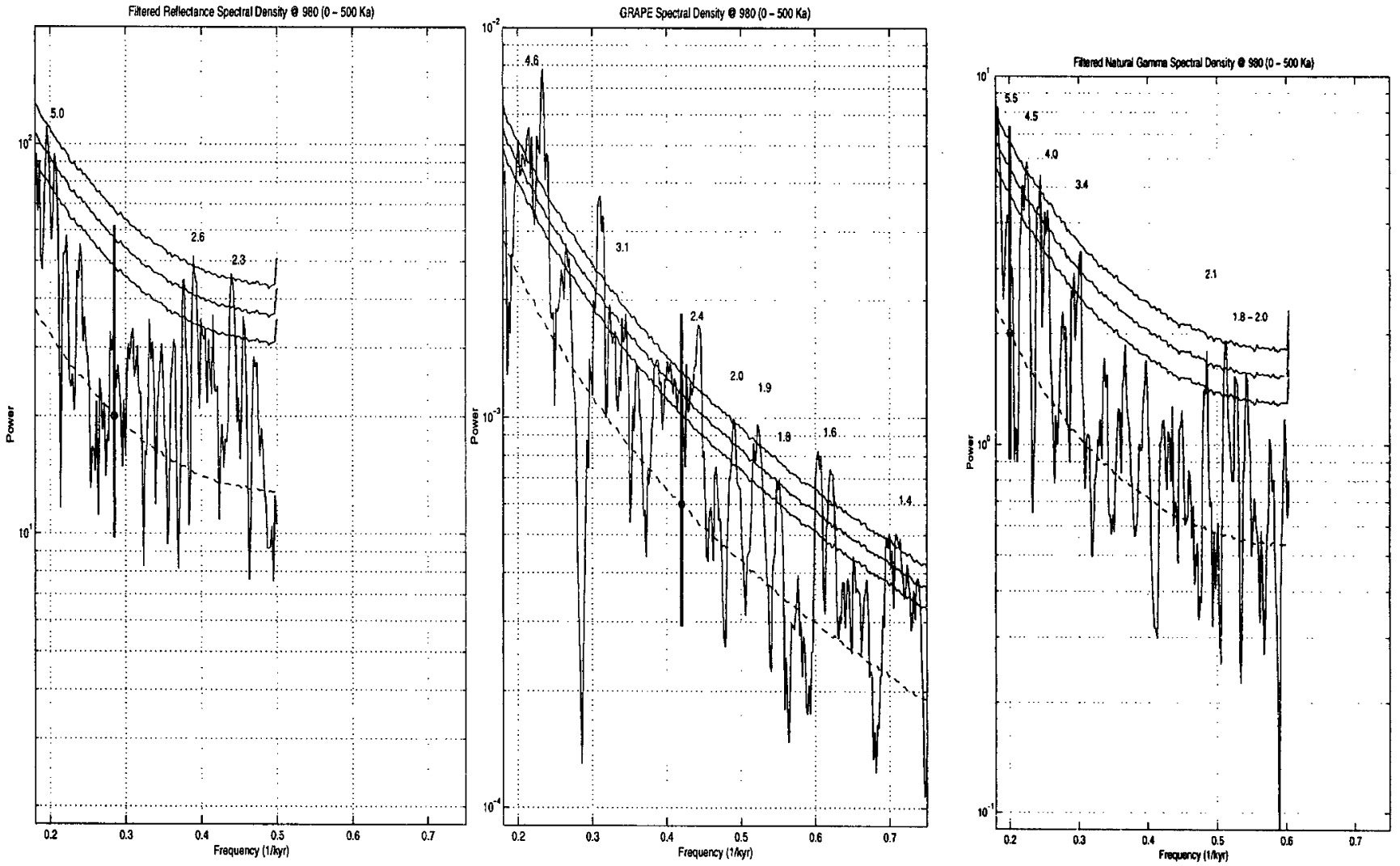

Figure 2.2 Spectral Reflectance (a), GRAPE (b), and Natural Gamma (c) log-linear spectra over the 0 to 500 Ka interval at Site 980.

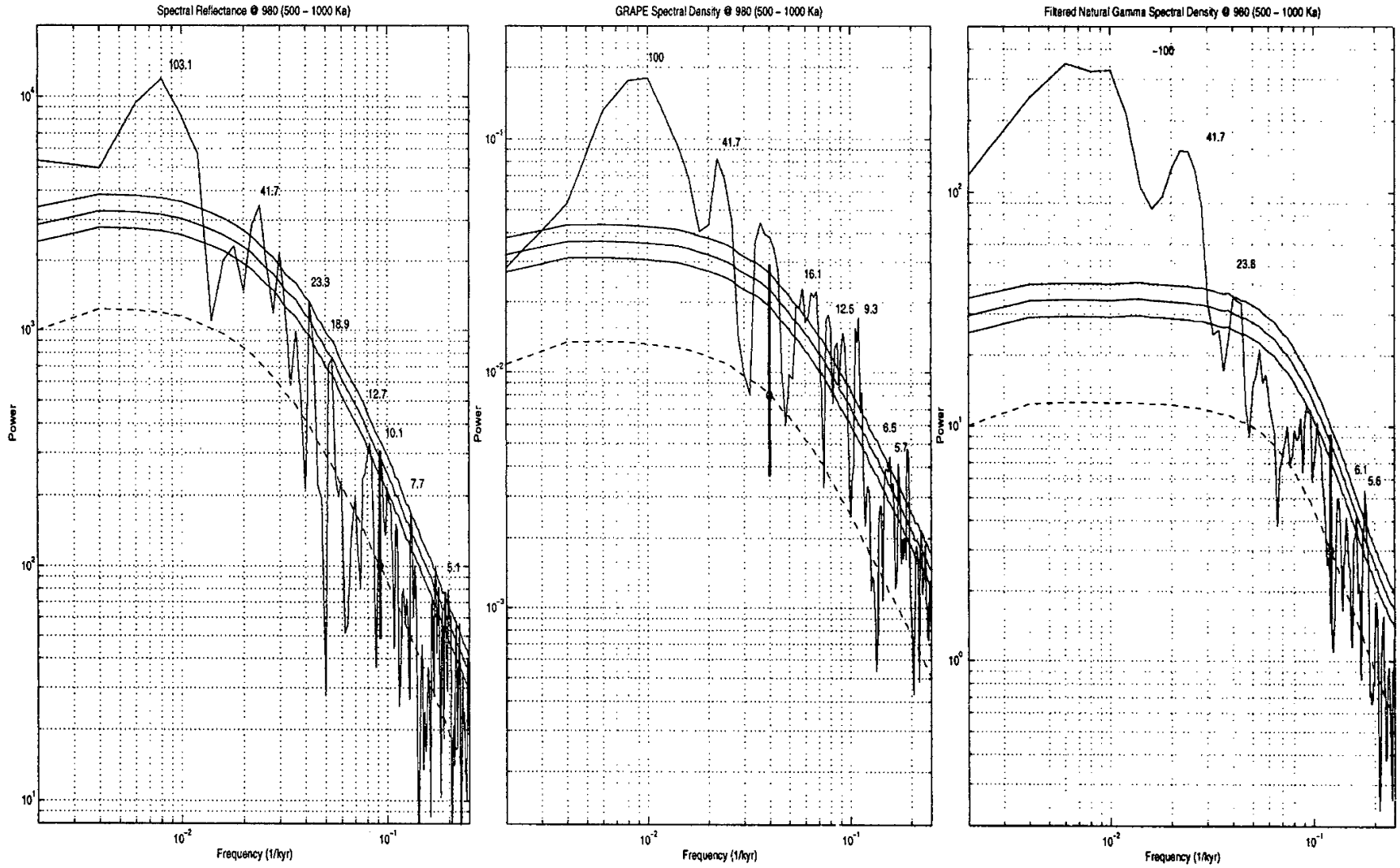

Figure 2.3 Spectral Reflectance (a), GRAPE (b), and Natural Gamma (c) spectra over the 500 to 1000 Ka interval at Site 980.

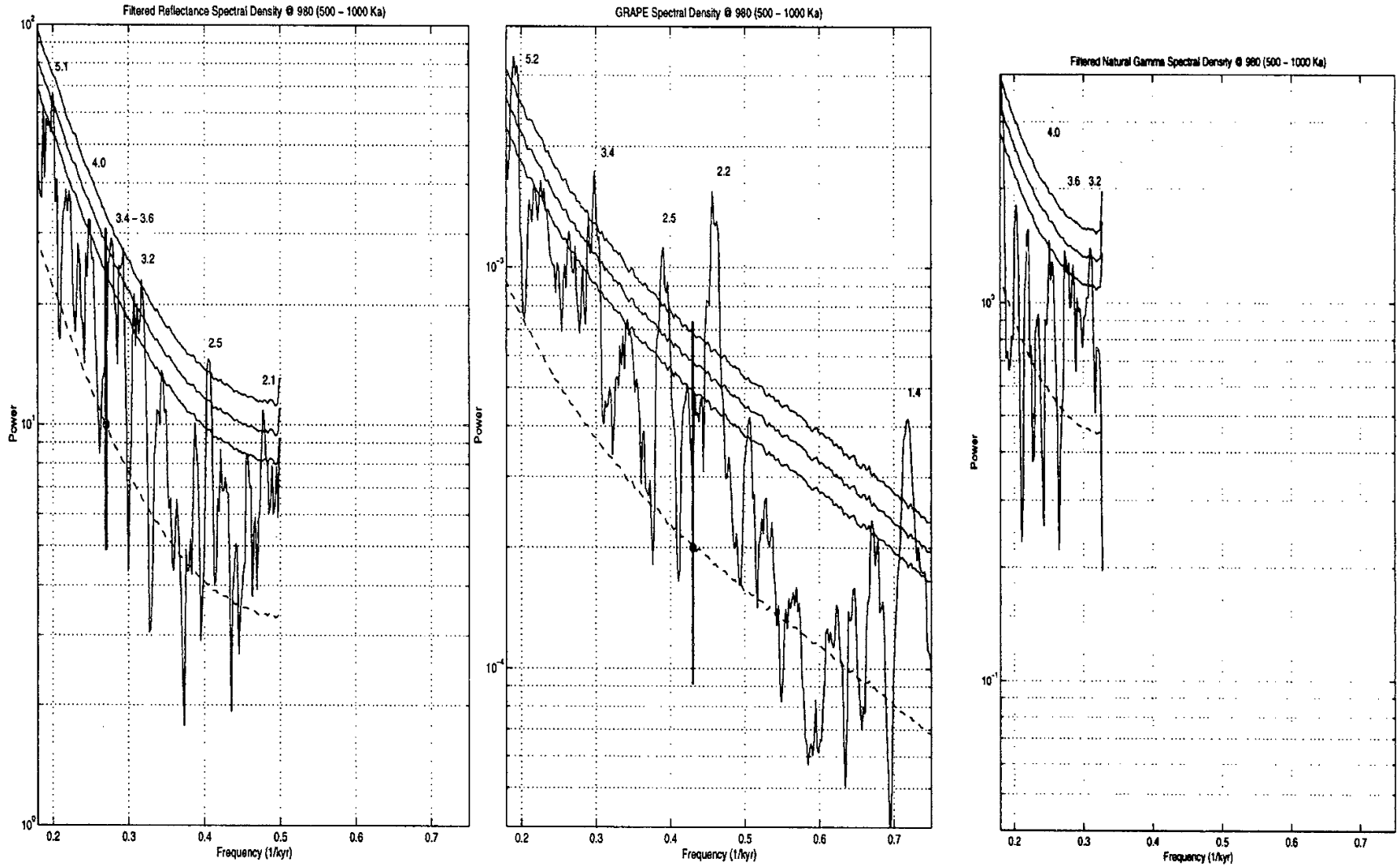

Figure 2.4 Spectral reflectance (a), GRAPE (b), and Natural Gamma (c) spectra over the 500 to 1000 Ka interval at Site 980.

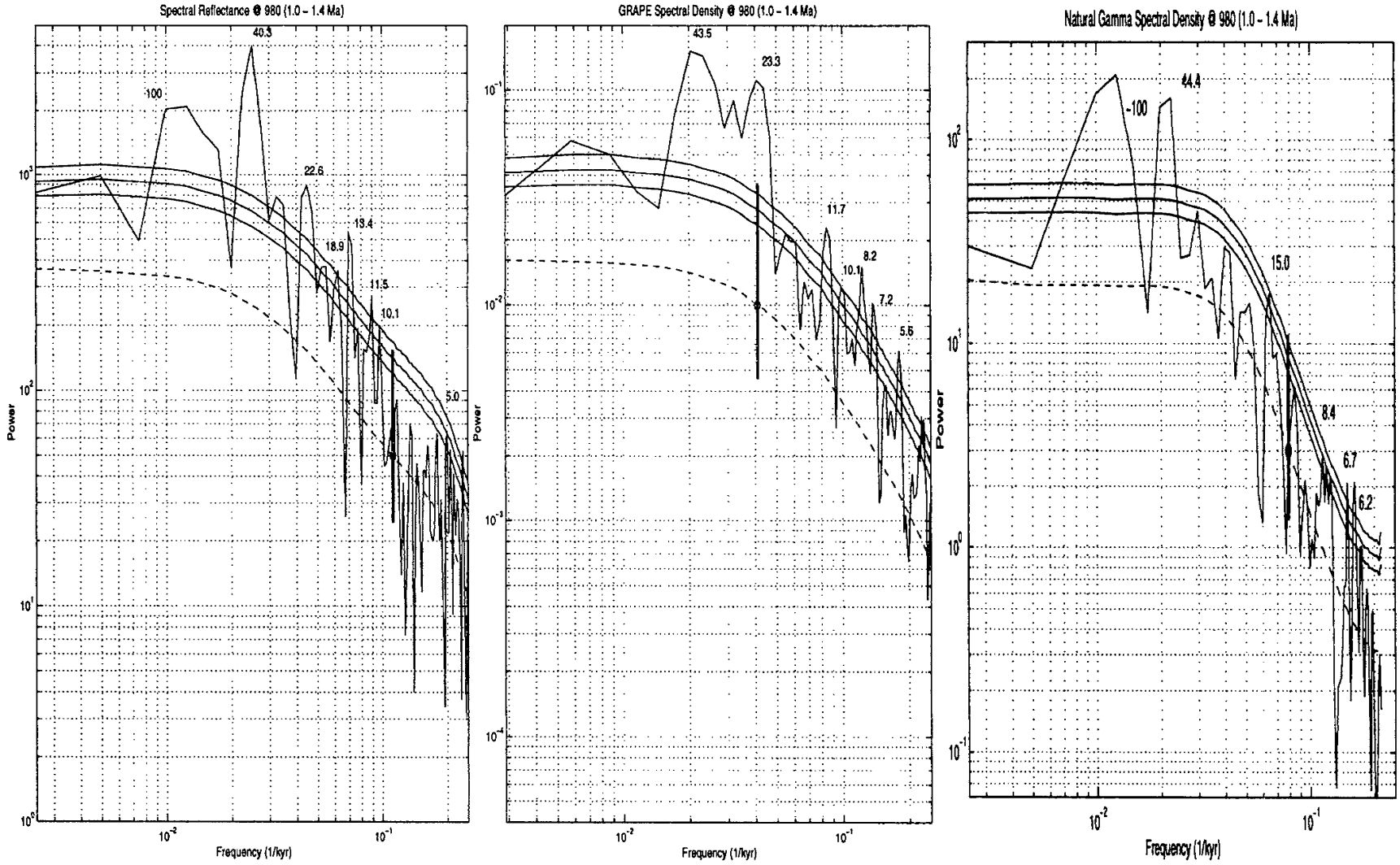

Figure 2.5 Spectral Reflectance (a), GRAPE (b), and Natural Gamma (c) power density spectra over the 1.0 to 1.4 Ma interval at Site 980.

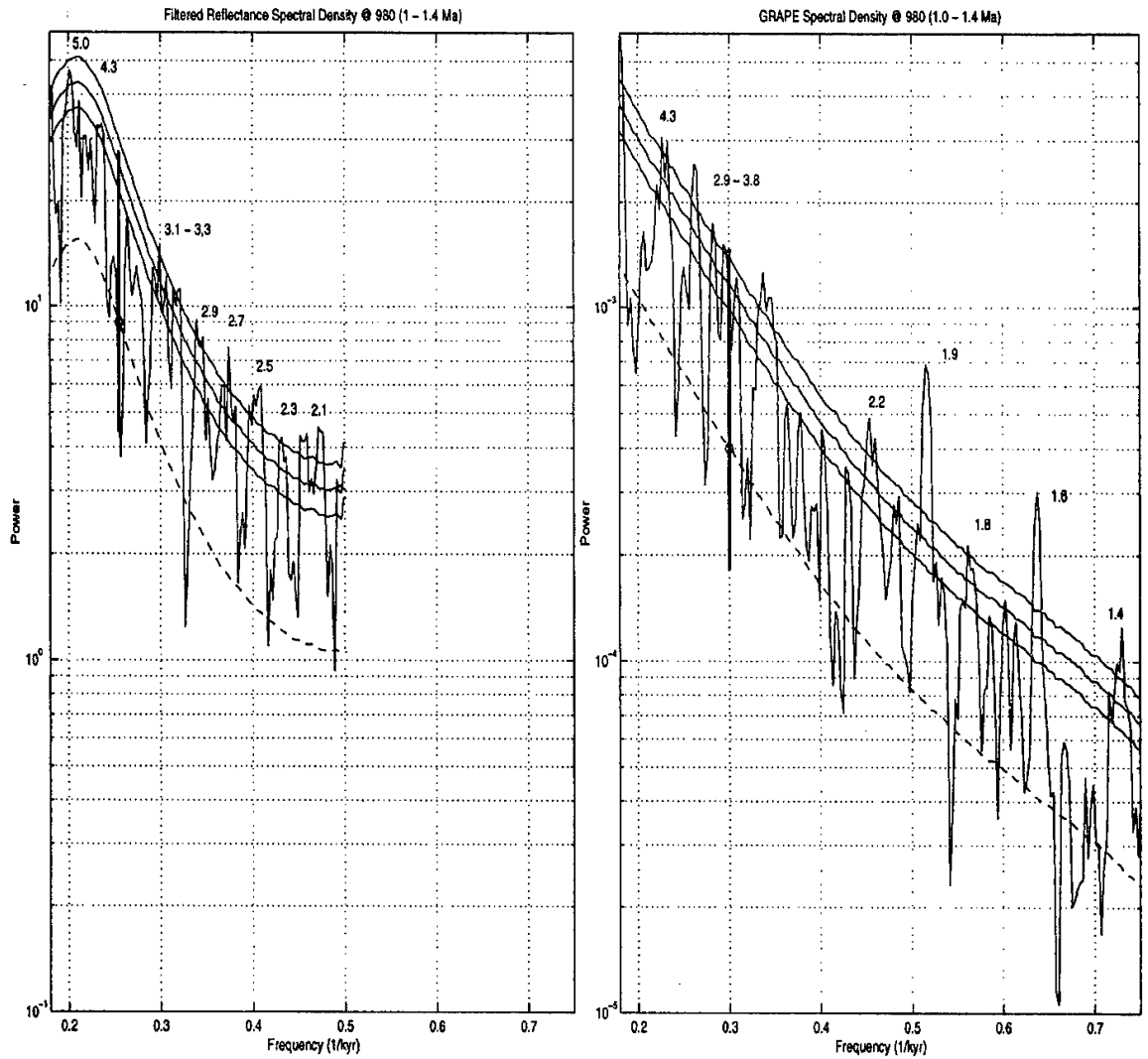

Figure 2.6 Spectral Reflectance (a) and GRAPE (b) over the 1.0 – 1.4 Ma interval at Site 980. No Natural Gamma plot is displayed because the sampling interval was not great enough to perform spectral estimation within this period band.

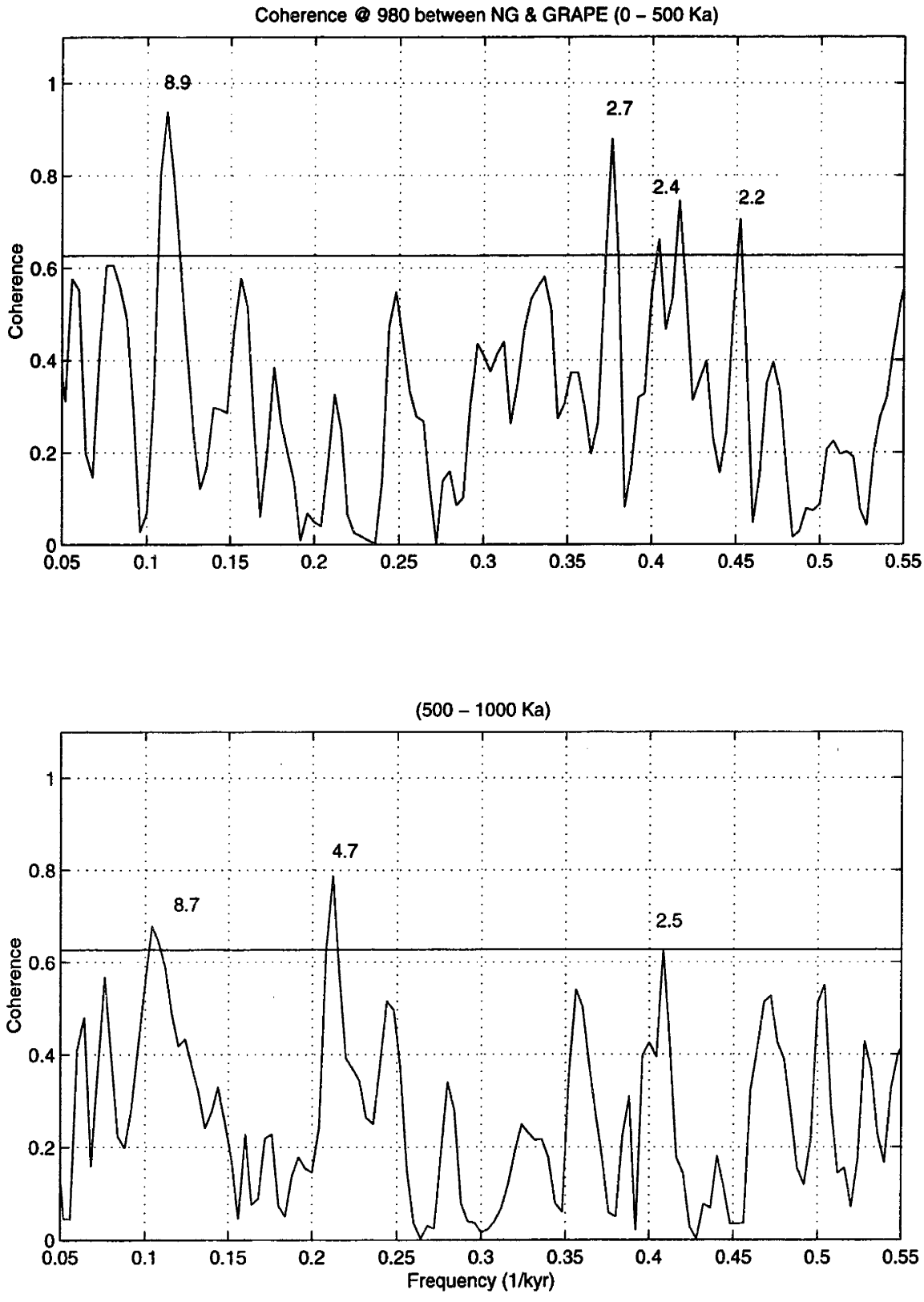

Figure 2.7 Coherence plots between Natural Gamma and GRAPE at Site 980 over the 1.4 Ma interval. The 95% confidence level for non-zero coherence is shown as well.

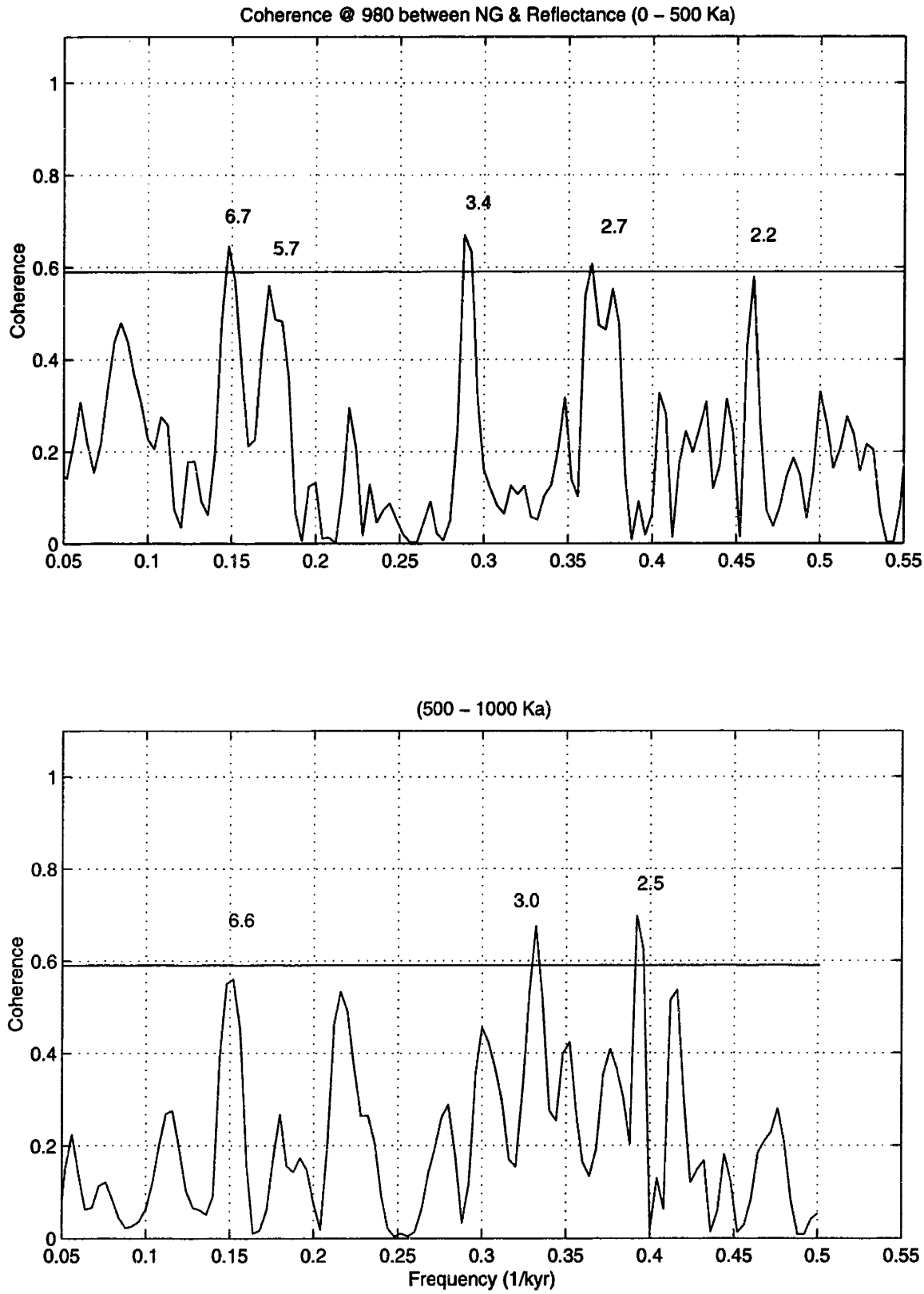

Figure 2.8 Coherence plots for Natural Gamma and Spectral Reflectance at Site 980 over the 1.0 Ma interval.

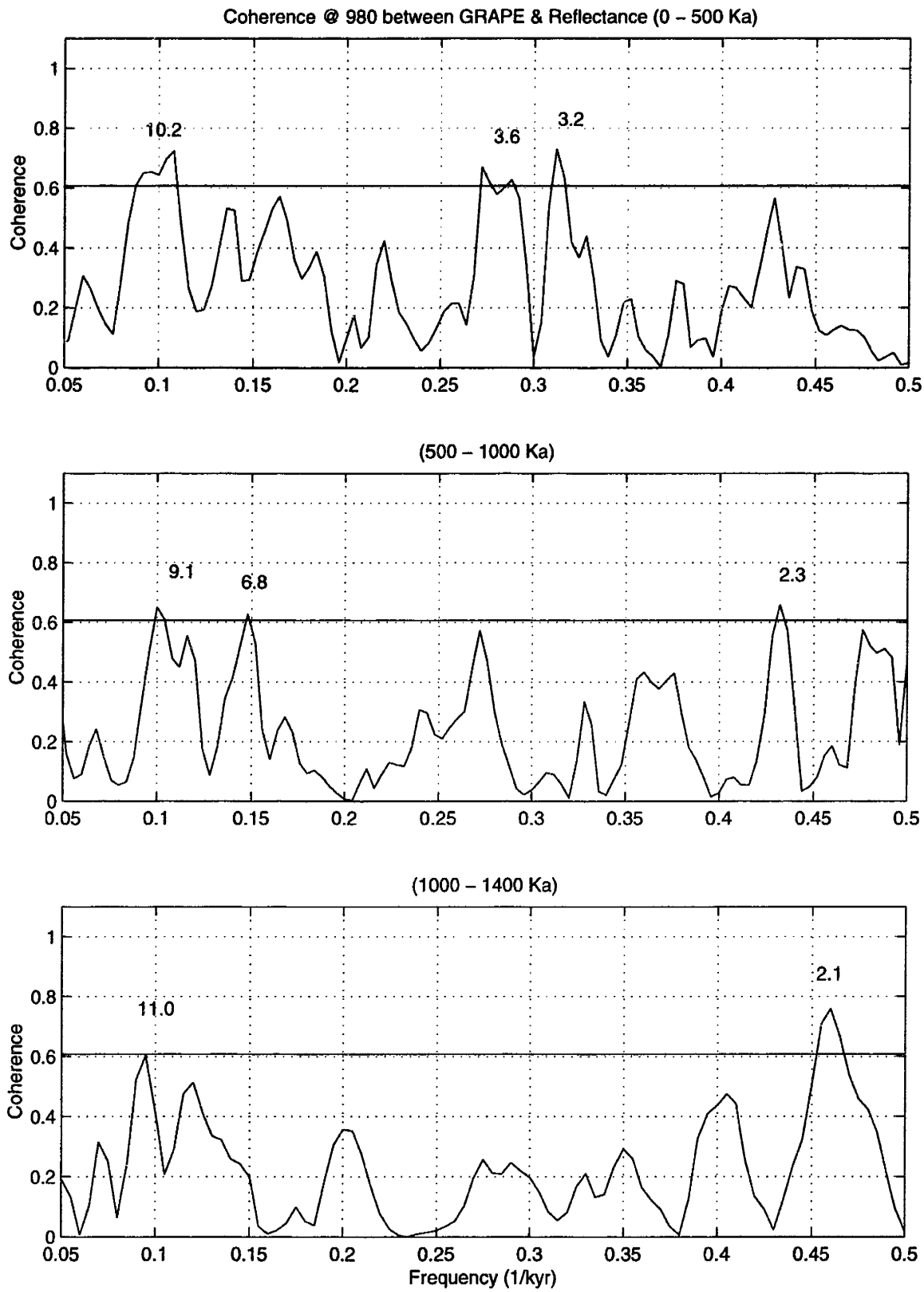

Figure 2.9 Coherence plots between Spectral Reflectance and GRAPE at Site 980 over the 1.0 Ma interval.

spectra and can also be found in the reflectance signal beyond 500 Ka (Figure 2.1 – 2.6). Its strongest signature is found in the GRAPE spectra (>>99% confidence).

The GRAPE spectral density displays a persistent signal at ~1.4 kyr (Figure 2.2.b, 2.4.b, and 2.6.b). Unfortunately, it is the only proxy studied at Site 980 that has a high enough sampling interval to resolve the power spectrum at this frequency. Thus, even coherence tests, which might help in deriving a masked signal, will be of no use in ascertaining the presence of this pacing in the other two proxies.

Site 983

It is from the vantage point of Site 980 that we may now proceed to the analysis of Site 983. In particular, are the millennial-scale periodicities found in the proxies at Site 980 found at Site 983 and, if so, are they due to climate variability, ice sheet dynamics, an oscillating ocean current strength, etc?

The Heinrich regime at Site 983, here roughly defined as the frequency range from ~15 to 5 kyr, is difficult to characterize across proxies and age intervals (Figure 3.1 – 3.9). The natural gamma signature within this regime is typically weak and displays sporadic peaks in spite of high-pass filtration (Figure 3.1.c, 3.3.c, and 3.5.c). Both magnetic susceptibility and GRAPE display a variety of statistically significant peaks according to both confidence intervals but it is difficult to formulate a consistent pattern (Figure 3.1(a,b), 3.3(a,b), 3.5(a,b)). There is some coincidence between MS and GRAPE over the 0 – 500 Ka interval at a pacing of ~13.1 kyr. This oscillation also appears in the 1 – 1.4 Ma in both the natural gamma and GRAPE proxies (Figure 3.5(b,c)) but not within the magnetic susceptibility spectral density, which displays only one significant periodicity over that interval (> 95% via the NBE) (Figure 3.5.a). Again, the coherence plots (Figure 3.7 – 3.9) do not display a strong degree of correlation at the ~13 kyr period but rather a potentially wide band of coherence ranging from ~7.8 – 13.2 kyr (especially coherence with MS). This could be interpreted as harmonic combinations of orbital periodicities where these proxies are responding with different degrees of variance. That could explain why we see some case for coherence in the broad band sense but no case in the narrow. Furthermore, it is not clear whether these harmonics should be interpreted as a numerical artifact or a true harmonic response in the climate. Therefore, neither can we say these frequencies represent Heinrich-type events or harmonic combinations.

However, it is clear that, no matter what their origins are, these periodicities do not display a standard pacing over long time intervals (Heinrich, 1987; Bond, 1993; Alley and MacAyeal, 1994). Rather, the coherence and spectral estimations suggest that (if this regime *is* real) there is considerable modulation in the frequency (and possibly within the amplitude) domain. Perhaps the use of shorter intervals and/or broad band filtration for spectral estimates would verify this hypothesis.

Periodicities of ~6.5 to 8.1 (the classic Heinrich interval) kyr appear to be a common feature to all proxies (Figure 3.1(a-c), 3.3(a-c), 3.5(b,c)). These periodicities are common to all three proxies over the 0 – 1.0 Ma interval and the GRAPE and natural gamma spectra also display this pacing over the 1.0 – 1.4 Ma interval. Coherence plots display these periodicities, albeit sporadically. Once again, we are only able to say that no persistent narrow band frequencies are present within this regime and that the broad band spectrum may contain a significant concentration of power. If this regime indicates Heinrich-type behavior (i.e., massive ice discharge events) it could be that GRAPE displays a *trough* associated with the influx of terrigenous material, and a peak associated with the ambient accumulation of biogenic carbonate material. Thus, we would see a periodic signal roughly 180° out of phase with the natural gamma and magnetic susceptibility profiles. Isolation of these frequencies in an attempt to assess their phase relationship can be performed but time did not permit this analysis.

As at Site 980, there is some evidence of ~4.9 – 5.2 kyr oscillations. It is strongest in the magnetic susceptibility record (>>99% confidence according to the NBE method but only marginally significant according to the χ^2 confidence interval) (Figure 3.2.a and3.4.a) but is also weakly present in the other two proxies (Figure 3.2(b,c), 3.4(b,c), and 3.6(b,c)). Notably, it is a very weak signal within the natural gamma spectral density (>95% [NBE] in the 0.5 – 1 Ma interval and >90% [NBE] in the 1.0 – 1.4 Ma interval). This situation is very similar to that found at Site 980, namely the weakest signature occurs in the natural gamma profile. Coherence tests show a total lack of correlation between proxies in this frequency band. Thus, while spectral reflectance at Site 980 displays a potentially significant band of oscillations centered at ~5.0 kyr, there is no compelling evidence to suggest its presence at Site 983. It should again be stressed

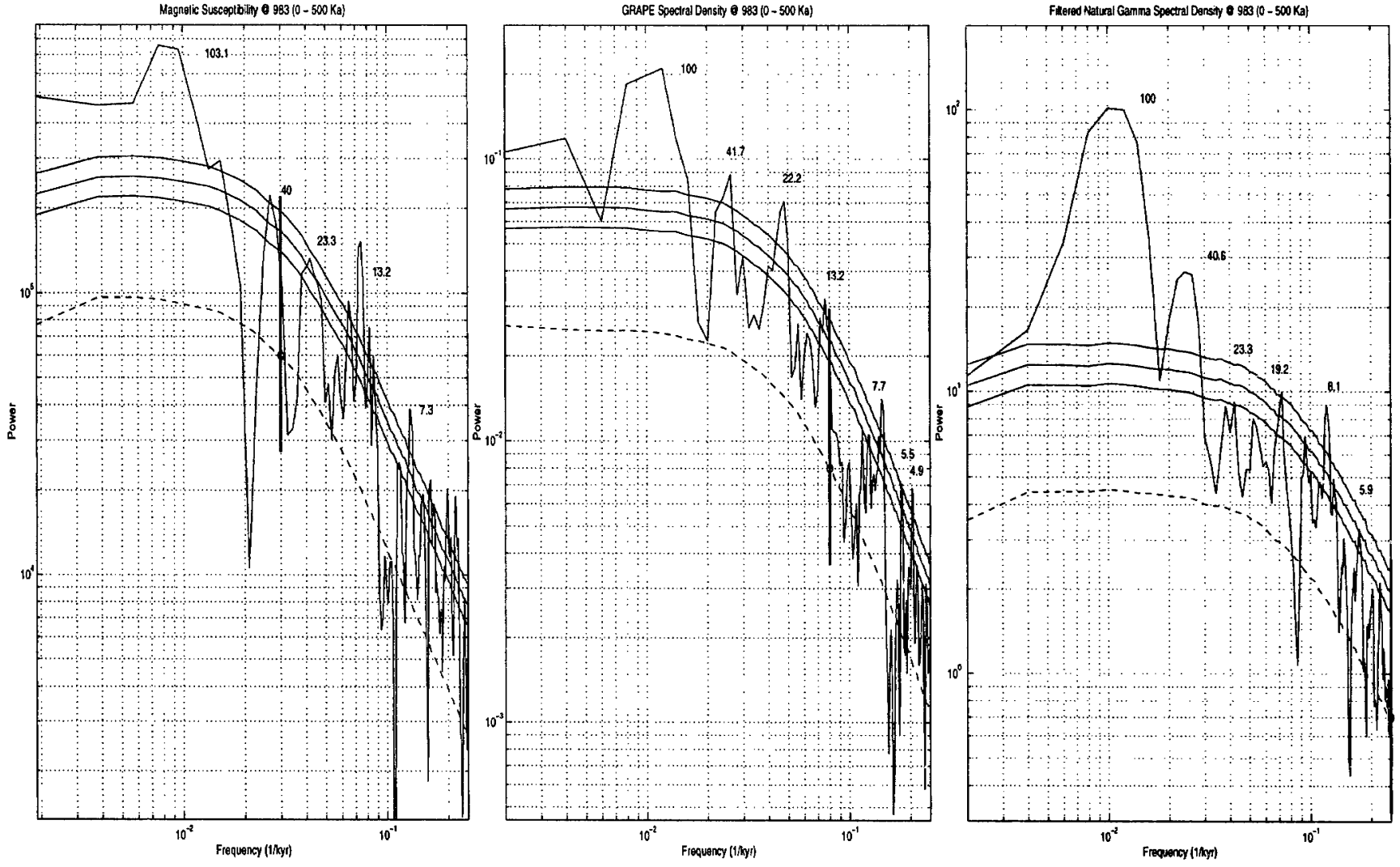

Figure 3.1 Magnetic Susceptibility (a), GRAPE (b), and Natural Gamma (c) spectral density plots over the 0 to 500 Ka interval at Site 983.

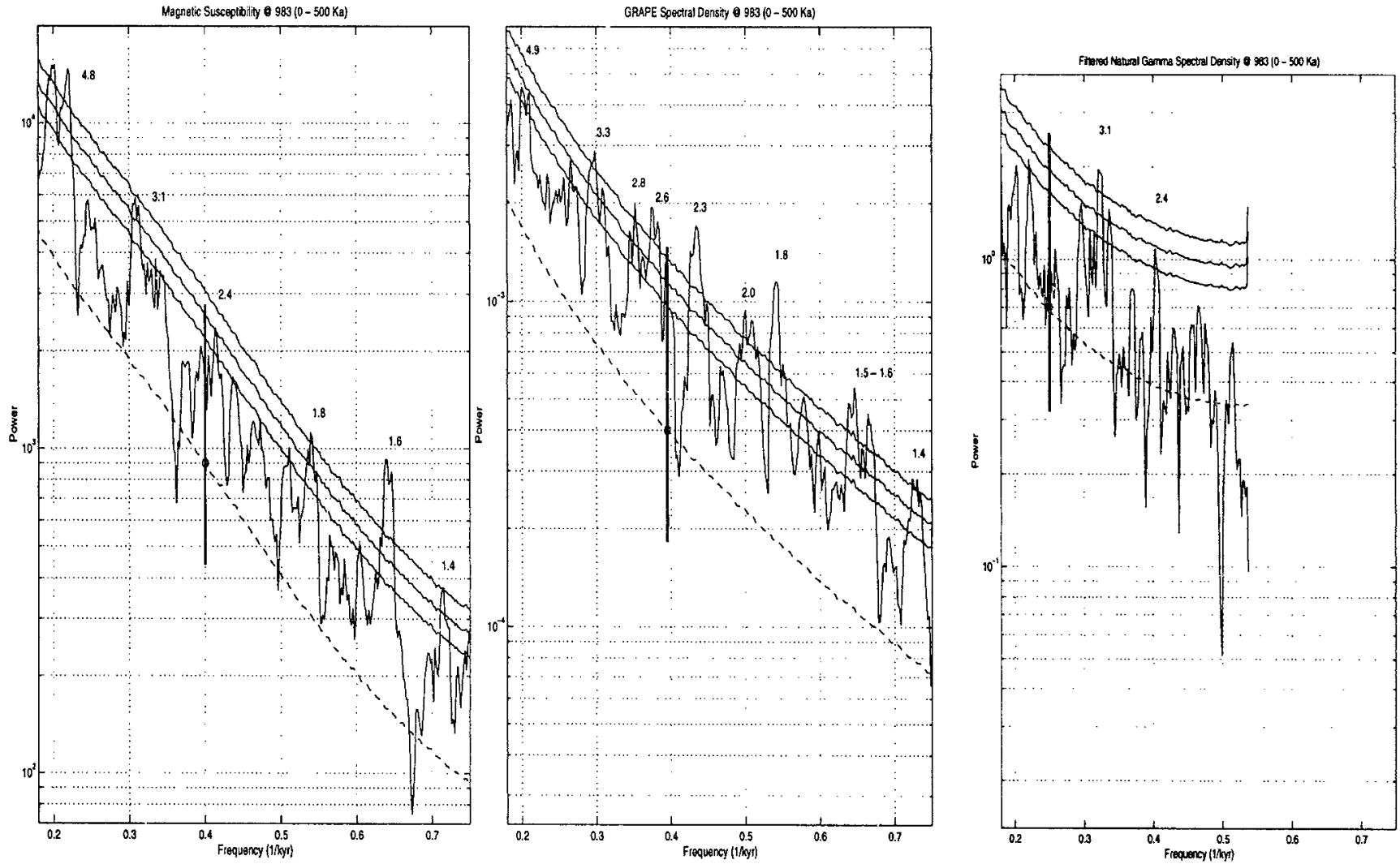

Figure 3.2 Spectral density plots for Magnetic Susceptibility (a), GRAPE (b), and Natural Gamma (c) over the 0 to 500 Ka interval at Site 983.

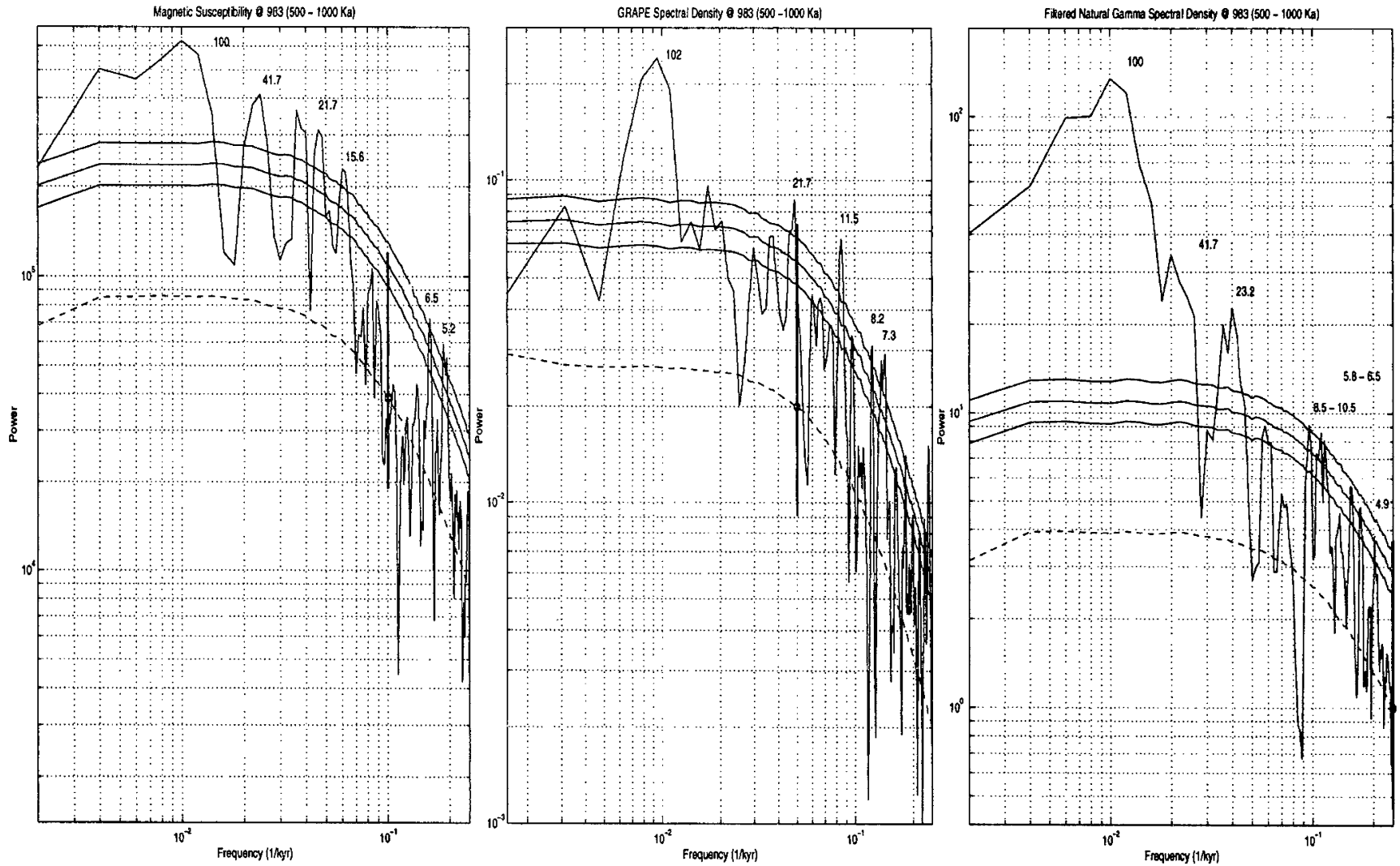

Figure 3.3 Magnetic Susceptibility (a), GRAPE (b), and Natural Gamma (c) spectral densities over the 500 to 1000 Ka interval at Site 983.

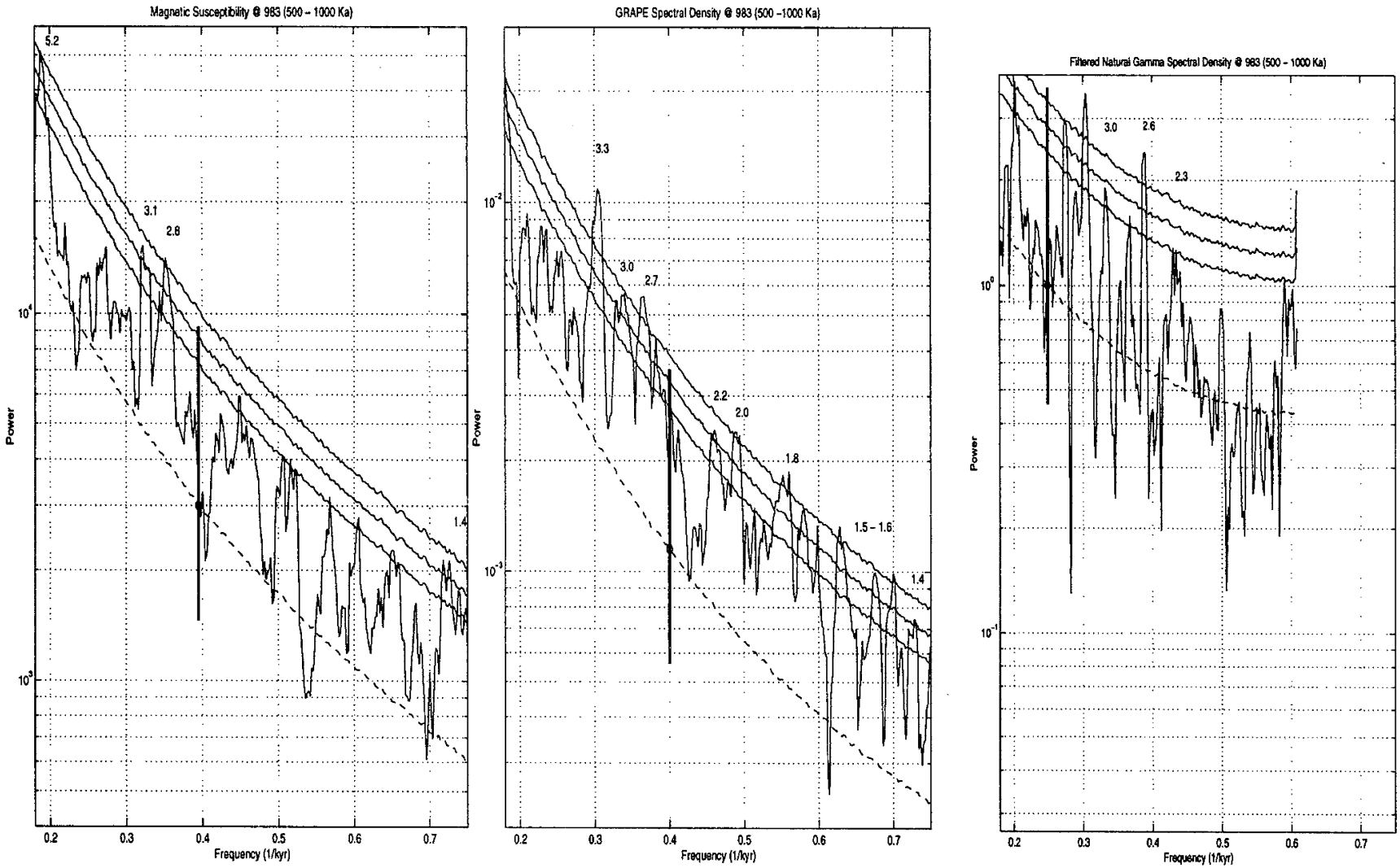

Figure 3.4 Log-linear spectra for Magnetic Susceptibility (a), GRAPE (b), and Natural Gamma (c) over the 500 to 1000 Ka interval at Site 983.

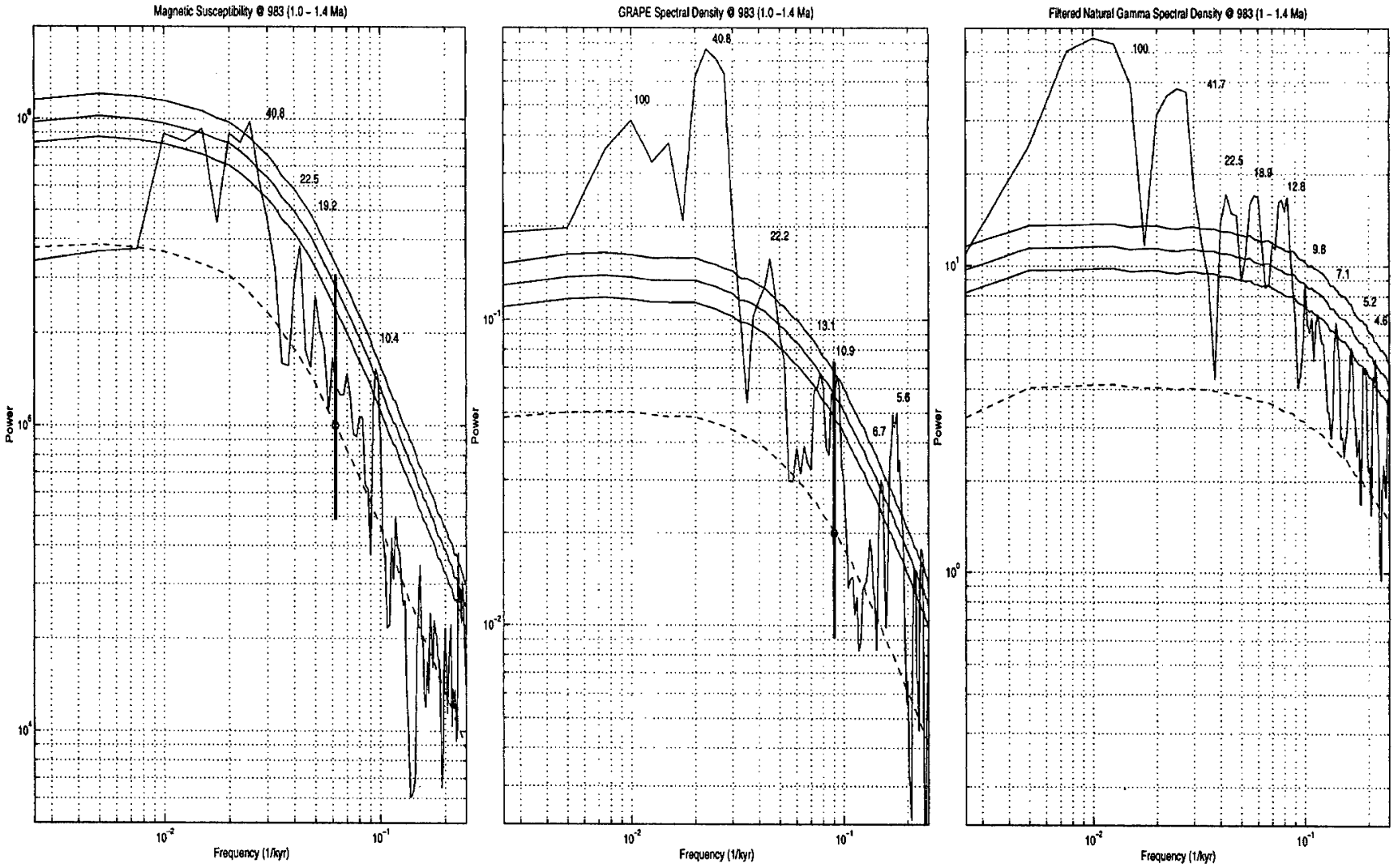

Figure 3.5 Magnetic Susceptibility (a), GRAPE (b), and Natural Gamma (c) spectra over the 1.0 to 1.4 Ma interval at Site 983.

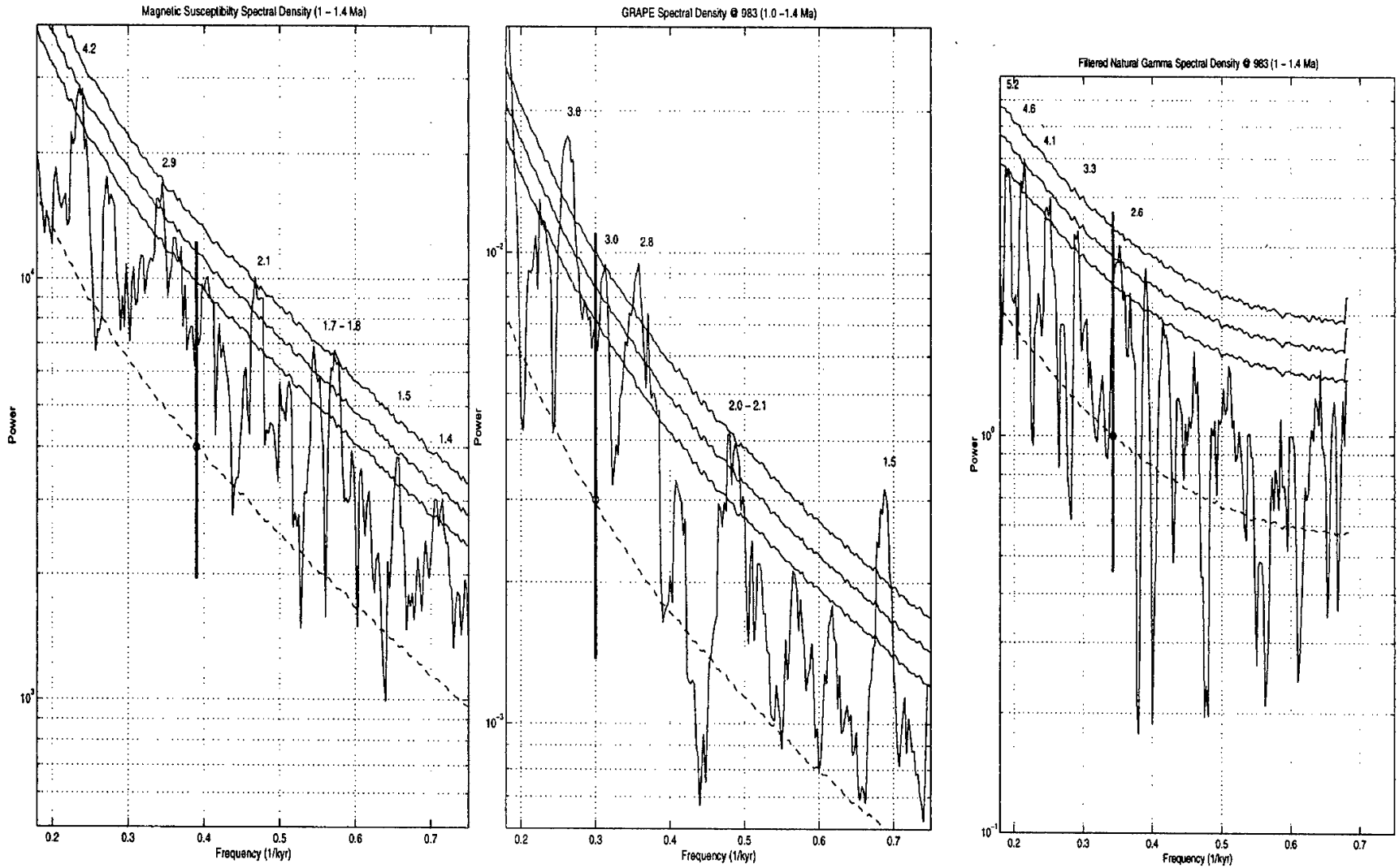

Figure 3.6 Magnetic Susceptibility (a), GRAPE (b), and Natural Gamma (c) over the 1.0 to 1.4 Ma interval at Site 983.

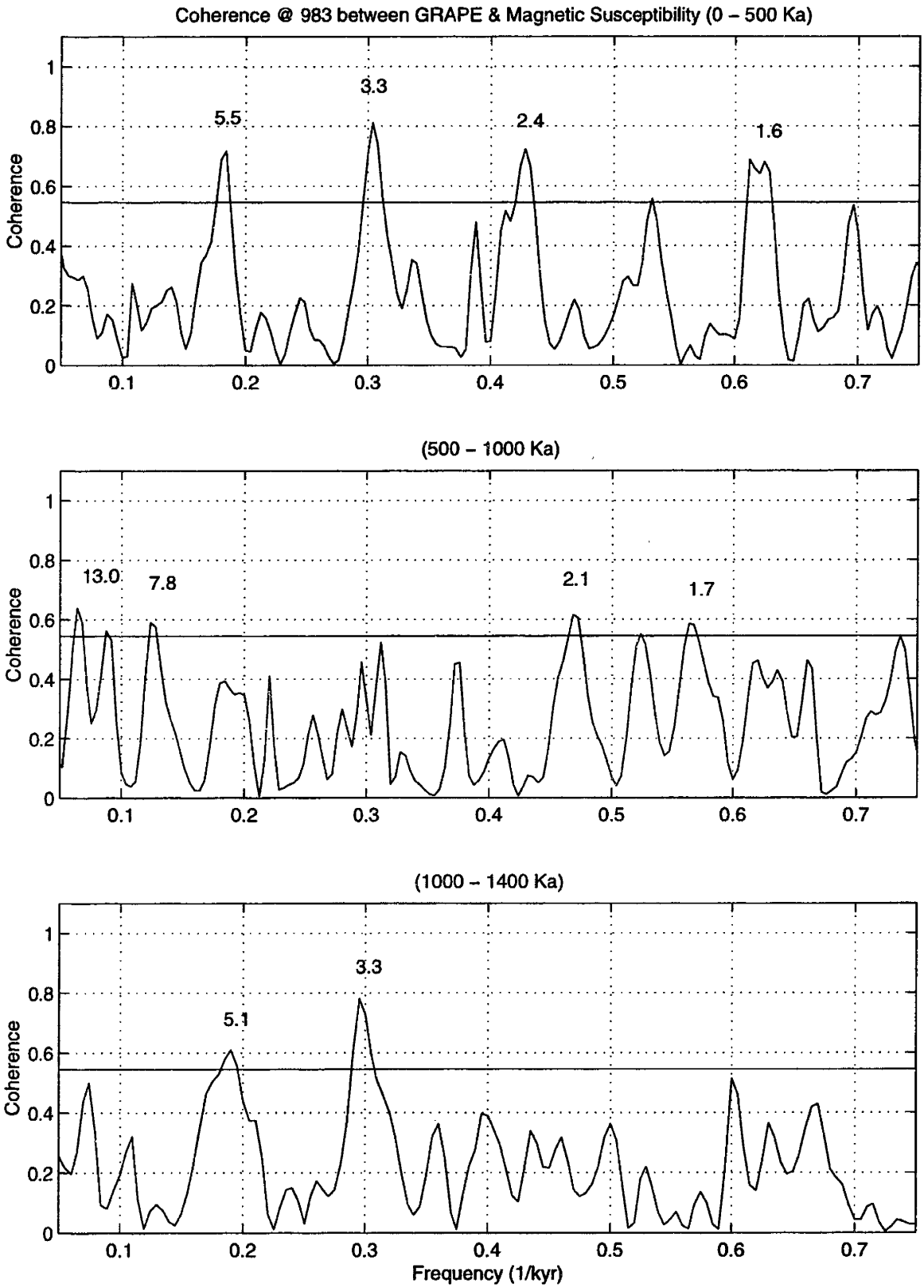

Figure 3.7 Coherence between GRAPE and Magnetic Susceptibility at Site 983 over the 1.4 Ma interval.

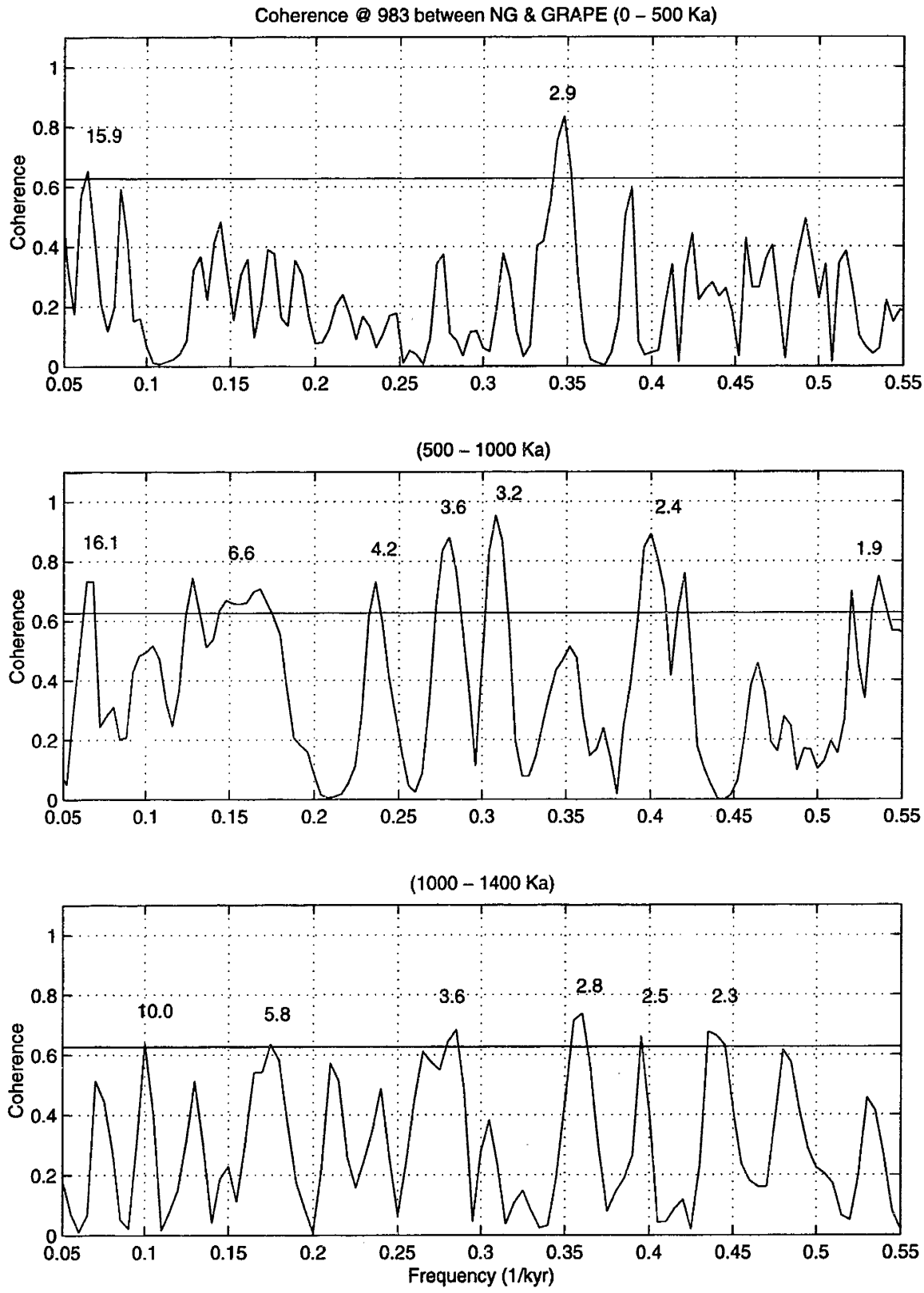

Figure 3.8 Coherence between GRAPE and Natural Gamma at Site 983 over the 1.4 Ma interval.

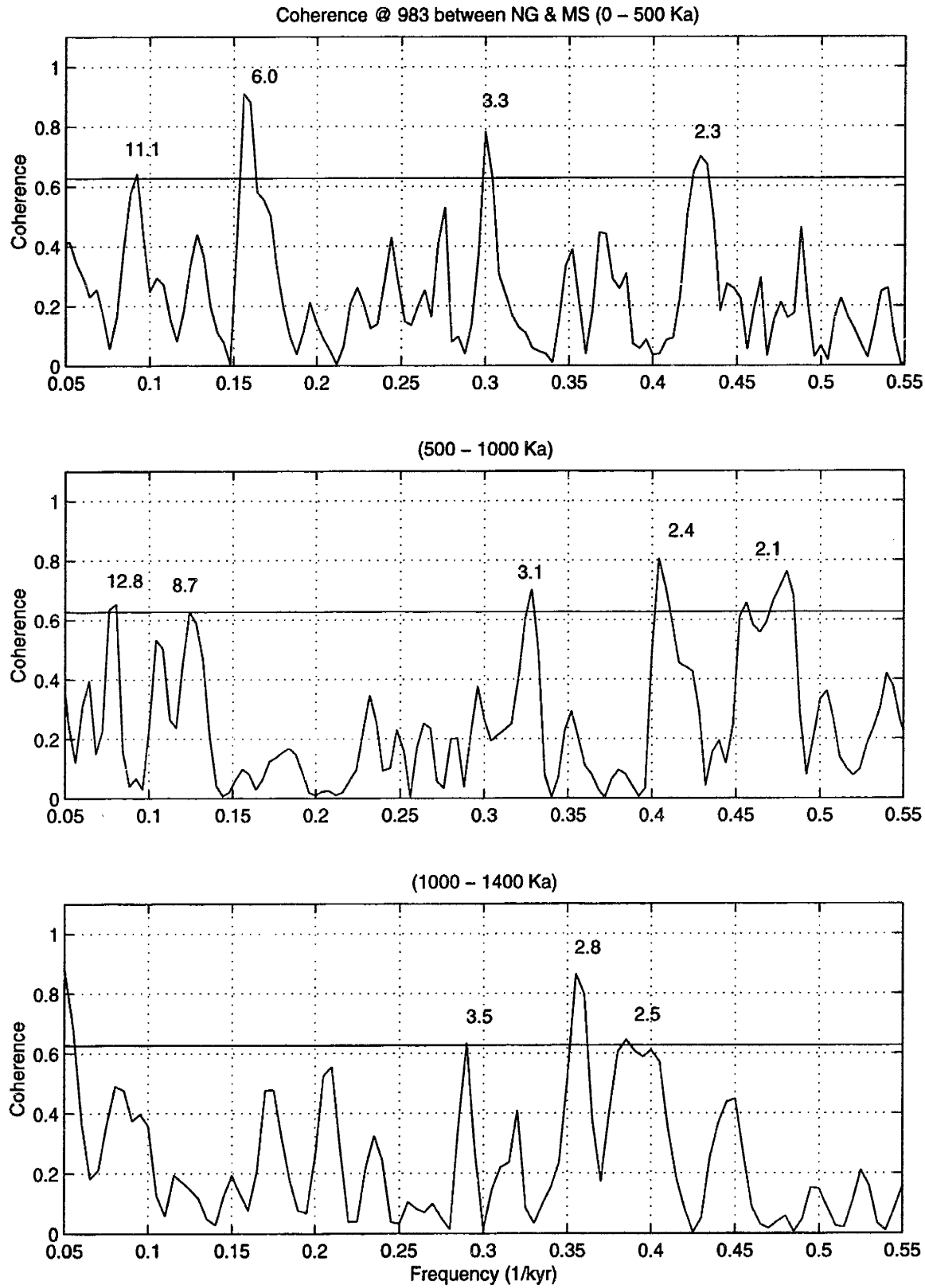

Figure 3.9 Coherence between Magnetic Susceptibility and Natural Gamma at Site 983 over the 1.4 Ma interval.

that we are considering these periodicities in the narrow band sense. Formal broad band analysis must be conducted to verify the findings of this paper.

Within the Dansgaard-Oeschger regime at Site 983, the most prominent peaks occur at ~2.7 – 3.3 kyr. This frequency band can be found in all proxies over the length of the entire 1.4-myr interval (Figure 3.2, 3.4, and 3.6). The most powerful signature is found in the GRAPE spectra where all incidence of this periodicity exceeds the confidence levels of both the NBE and the standard χ^2 methods. Both natural gamma and magnetic susceptibility display this pacing at no less than 95% confidence (NBE) as well. The coherence plots display consistent correlation between all three proxies as well. In fact, the coherence plots suggest that narrow band correlations exist between all three proxies within this frequency regime. This is a somewhat startling find. It suggests both that the age-model may be accurate to this degree of resolution and that there is a real, narrow band oscillation being recorded in all three proxies at Site 983.

There is also considerable incidence of periodicities ranging from ~1.5 – 2.1 kyr and ~1.4 kyr, which are evinced in the magnetic susceptibility and GRAPE spectra (Figure 3.2(a,b), 3.4(a,b), and 3.6(a,b)). Unfortunately, the sampling interval for natural gamma does not allow for comparison with the other two proxies. Again, the coherence plots between MS and GRAPE (Figure 3.7) suggest that there is narrow band coherence centered at ~1.6 kyr that ranges from 1.4 to 2.0 kyr. Two points should be made concerning this discovery. The χ^2 confidence levels suggest that this period band may be only marginally significant and the 95% confidence test for non-zero coherence may simply show a random fluctuation (as we expect to see at least 5% of the points found in a coherence plot that exceed the 95% level). Nonetheless, this is a compelling discovery that warrants closer scrutiny in the future.

At such high frequencies, we must seriously consider the contention that the age-model obstructs proper analysis. Indeed, these periodicities are determined under the assumption that the sedimentation rate is constant between tie points in the age-model. If the sedimentation rate does vary, we may arrive at entirely erroneous results. Thus, caution should be exercised when considering frequencies within this period band. However, evidence for narrow band coherence between proxies indicates that the age-

model may be sufficiently resolved. Contrarily, these coherences may actually derive *from* age-model inaccuracies, but this seems improbable.

Cross-site coherence

To this point, we've only considered spectra and coherence relative the proxies found at a single site. It is also informative to take a look at the coherence between the same proxy at two sites. This may lead to a better understanding of the physical processes recorded in the pelagic sediment at these two sites as well as in helping us identify the various sedimentary components at Site 983. Natural gamma and GRAPE are the two proxies common to both sites studied. Obviously, we expect these two proxies to respond to the same inputs, namely terrigenous and carbonate inputs respectively. Therefore, cross-site comparison of these two proxies may provide the greatest insight into common periodicities and sedimentary inputs.

The Heinrich-regime coherences for natural gamma and GRAPE displays only one coherent regime centered at ~13.8 – 14.1 kyr over the 0 - 500 Ka interval. Also, the shape of the coherence plots within this regime are similar looking. Thus, while we obviously cannot conclude that there is a significant narrow band frequency common to these two sites (for these two proxies), there is some evidence that they both may be responding similarly to some physical process, albeit only very weakly. When compared to the power density plots of natural gamma and GRAPE (Figure 2.1(b,c), 2.3(b,c), 3.1(b,c), and 3.3(b,c)), the coherence found within this frequency band is not surprising. Recall from earlier results that both sites seem to be displaying some concentration of variance within the broad frequency regime. However, neither the natural gamma nor the GRAPE spectral estimations displays significant frequencies centered at ~14.0 kyr. Thus, it is only clear that no narrow band frequencies are common to these two sites within this regime.

The GRAPE cross-site coherence (Figure 4.1) is actually surprisingly devoid of strong coherence. There is some indication of coherence at ~1.4 – 1.6 kyr over the 500 – 1000 Ka interval, which is in agreement with the spectral estimations. Also, there is some coherence at ~3.0 and 2.2 kyr between sites (for GRAPE), which is again in agreement with the spectral estimations. That there is not wider coherence between GRAPE at these two sites is surprising. Certainly, it demonstrates the fact that there are

few or no instances of narrow band type oscillations common to these two records. However, for example, the ~1.4 – 2.0 kyr band is a commonly significant regime within the GRAPE spectral estimations. Then why do we not see this fact reflected in the coherence plots? It is unclear whether there is some type of error in the method used to generate the coherence or confidence intervals for this plot. This seems like the most likely explanation, however.

Natural gamma cross-site coherence provides similar results as GRAPE, namely, there is hardly as much coherence as we would expect. There is some correlation between sites in the ~2.0 – 3.0 kyr band, which is in agreement with the spectral estimations. Again, this study would only suggest that there are definitely no narrow band oscillations common to both sites within the natural gamma data.

Discussion

Sub-orbital and millennial-scale cyclicity

The discovery of narrow band frequency regimes that are persistent across proxies and sites would be a strong indication that the climate does in fact display a highly structured signal similar to a ringing bell. The results of this analysis generally support our intuition about the nature of oscillations in the climate signal. Of course, a pure sinusoidal periodicity would be a very unusual discovery in the climate signal. The vast majority of the analyses conducted in this paper suggest that such oscillations do not exist. The only exception can be found at Site 983. The GRAPE and magnetic susceptibility profiles show persistent significant spectra ranging from ~1.6 to 3.3 kyr. The use of coherence functions to verify the existence of these periodicities provides compelling evidence that this frequency regime is faithfully recorded by both of these proxies. It is notable that Site 980 proxies and the cross-site coherences do not display any appreciable coherence at these periodicities.

We are left the task of trying to explain what may cause these results to arise. A variety of explanations present themselves. First, it could be that the age-model employed at Site 983 is simply under-resolved. If the sedimentation rate between tie points in the SPECMAP was variable at Site 983, then it could be that we are merely seeing a numerical manifestation of this fact. We may merely be witnessing the

concentration of variance within this period band due to incorrect interpolation of the sedimentation profile. However, persistent coherence between GRAPE and MS seems to rule out this hypothesis. Regardless of whether the age-model is adequate or not, we may infer that the GRAPE and MS data sets at 983 are responding similarly within this frequency band. This observation stems from the fact that the same age-model was used for all proxies at Site 983. Thus, even if the estimated concentrations of variance are incorrect (due to age-model limitations), it would be necessary that both data sets have similar time-domain profiles. Otherwise, we would not expect to see such a coherent concentration of variance under the same age-model (adequate or not).

Second, now that we have established that both MS and GRAPE must display similar profiles in the age domain (at these periods), we need to understand what if any mechanism would cause this to be so. From this point, we may posit a contrary hypothesis. Since GRAPE is a density-dependent proxy (bulk-wet density) and magnetic susceptibility is essentially a terrigenous-sensitive proxy, this frequency regime must be dominated by some type of rapid variation in the amount of terrigenous material deposited at Site 983. Thus, we would expect to see some type of phase relationship between these two proxies within this frequency band. Filtration would be useful in validating thus hypothesis. Furthermore, since Site 980 does not display such persistent coherence within this regime (nor do the cross-site coherences), we may surmise that this oscillation is unique to Site 983. This rules out a rapid ice rafting hypothesis since we would then see strong coherence at Site 980 as well (this hypothesis assumes that the age-models at *both* locations are adequate and that there are no surface current variations that would preferentially deposit more IRD at one location than another). Then, a tenable hypothesis is that the ISOW experiences periodic, narrow band oscillations at ~1.6 – 3.3 kyr. The ISOW current strength could vary from strong to weak and, in so doing, alter the composition of entrained sediments. Thus, assuming carbonate sediment is generally finer and less dense than terrigenous material, a slower ISOW would entrain carbonate material in a greater ratio relative to terrigenous material. During this phase of an ISOW oscillation, we would see a GRAPE peak and a MS trough. Then, during a more vigorous ISOW current, the ratio would be altered by the entrainment of more terrigenous material, altering the ambient mixture of the two (clearly we would see some reflection of

this in both proxies). The one glaring facet of this theory is that variations in current strength may also affect the sedimentation rate. This would contradict the original assumption upon which this theory is based. It is not known how sedimentation rates would vary as a function of current strength and sediment entrainment.

Lastly, the effects of aliasing should be addressed. While this hypothesis cannot be tested at present, it could be that this periodicity band derives from the aliasing of some very high-frequency oscillation that we cannot resolve.

While the Heinrich regime at both sites does not display any coherent narrow band frequencies, there does appear to be a considerable concentration of power within the ~8.8 – 11 kyr band. Future research should address this potential regime by employing heavier smoothing techniques. Presently, it is still unclear whether we should attribute this variance to classic Heinrich events as described by Alley and MacAyeal (1994) or Bond and Lotti (1995). Or, this period band may reflect harmonic combinations of Milankovitch periodicities (e.g. Ortiz et al., 1999). While the harmonic theory is very compelling, it is not known how it may be rigorously proven except by contrapositive methods (i.e. proof that other theories are wrong may imply that the harmonic theory is right). A more rigorous approach to the harmonic theory must be implemented.

Age-model concerns

While it was originally hoped that we could make some assessment of the age-model resolution issue as regards the study of sub-orbital and millennial scale climate variability, this assessment was implicitly method-dependent. In other words, if it was shown that there were coherent narrow band high-frequency oscillations common to all proxies and sites, we might be able to assert that the age-models were sufficiently resolved. However, with the exception of the ~1.6 – 3.3 kyr regime at Site 983 (discussed above), there is little evidence to suggest that the age-models are or are not adequate. It could be that the age-model used at Site 983 was sufficient for millennial-scale discussion while the one at Site 980 was not. Of course, this would be a rather unusual situation. Site 983 is thought to be four-component sediment profile, one of whose independent inputs is sediment transport by deep-sea currents (the ISOW). We

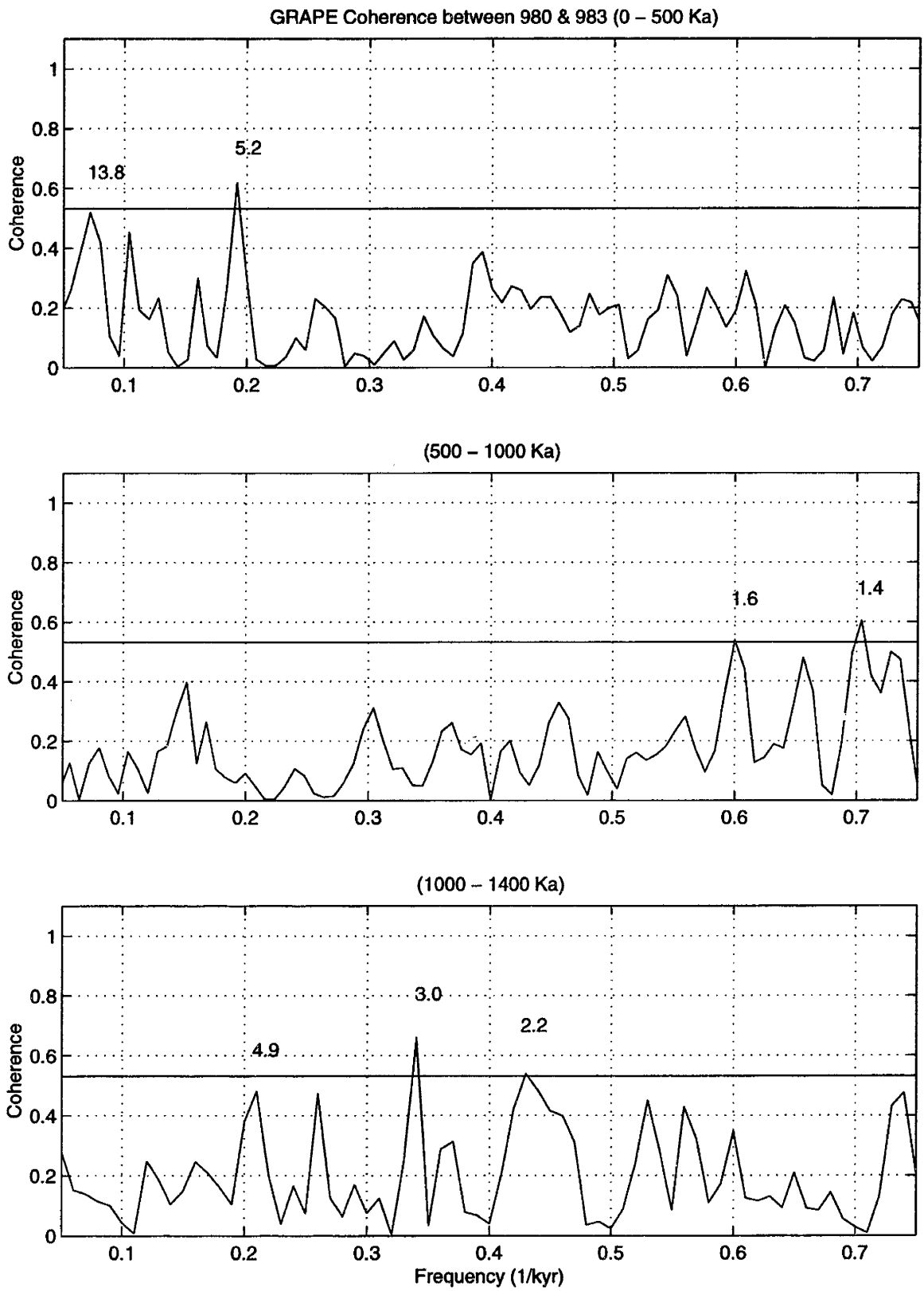

Figure 4.1 Cross-coherence for GRAPE data at Sites 980 and 983 over the 1.0 Ma interval.

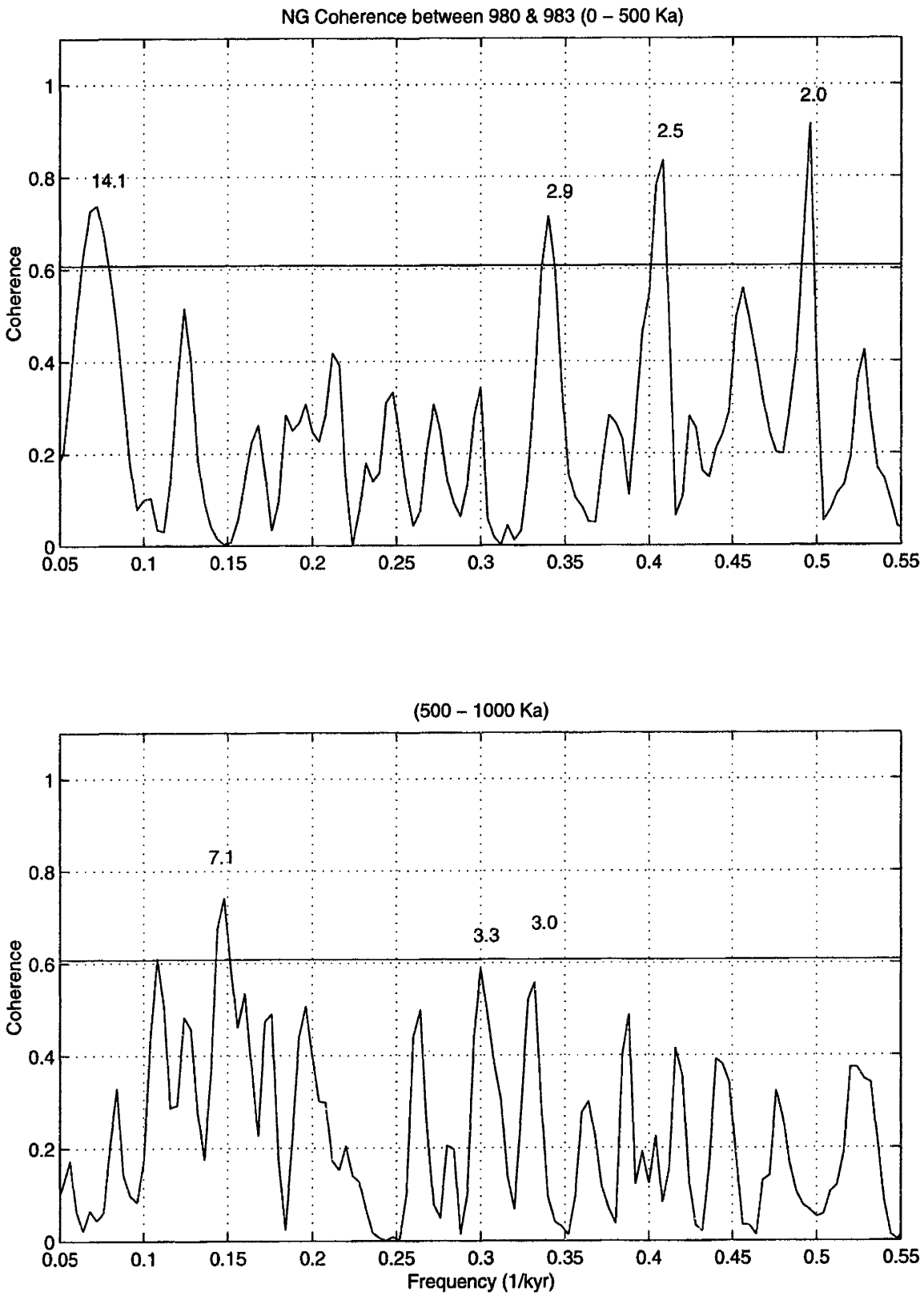

Figure 4.2 Cross-coherence for Natural Gamma data at Sites 980 and 983 over the 1.0 Ma interval.

might surmise that the age-model at Site 983 would be the poorer of the two if we assume that sedimentation rate is a function of variable current strength and sediment entrainment. Thus, while we do see strong coherence and spectra at ~1.6 – 3.3 kyr at Site 983, it would be premature to claim that age-models are sufficiently resolved to discuss high-frequency variations in the climate signal.

Future attempts to assess the adequacy of age-models should focus upon simple sedimentation profiles such as those found at Site 980. This reduces the number of variables we must consider when attempting to make our assessment. Furthermore, as is patently clear from this research, more heavily smoothed spectral estimates are in order. It is clear that no common line frequencies generally exist across sites or proxies. This fact makes age-model assessment impossible by the methods used in this paper.

Proxy robustness

The third thrust of this paper was to provide some assessment of the four proxies used, in consideration of their sensitivities to orbital and, more importantly, sub-orbital variations. The results of this analysis suggest that all proxies are sufficiently sensitive to Milankovitch oscillations. Natural gamma data appears to respond most strongly to oscillations within the orbital regime, which suggests that this proxy is particularly well suited for age-model construction/checking. However, the sampling frequency of the natural gamma data (~1000 year time steps) does not allow for the degree of resolution we may desire in the frequency domain (~1/2000 years, the Nyquist frequency).

On the other hand, both magnetic susceptibility and GRAPE demonstrate powerful and coherent sub-orbital spectra. Both of these proxies make excellent candidates for future research of sub-orbital variability recorded in deep-sea sediments. Spectral reflectance agrees widely with the magnetic susceptibility and GRAPE data over the sub-orbital regime. However, in this paper reflectance data did not provide the resolution necessary to discuss periodicities shorter than 2000 years (the Nyquist frequency). While this could theoretically be rectified simply by taking more frequent measurements along the sediment core, this may be impractical. Ortiz et al. (1999) provide an extensive explanation of the method used to acquire the spectral reflectance data, which I will not reproduce here. The point is that acquisition of the reflectance data is time-consuming and it may be impractical to collect a more densely sampled data set

while the research vessel is at sea. While shore-based sampling may be an alternative, it is not known how the spectral reflectance signal may be altered by drying and thermal/pressure expansion of the core samples. While GRAPE typically provided a degree of resolution sufficient to discuss periodicities down to 1.4 kyr, the data collection is again time-intensive (Boyce et al., 1976). As time is a commodity on board research vessels, the fact that GRAPE data collection is so time-intensive may make it undesirable in future work. Thus, magnetic susceptibility suggests itself as the best all-around proxy as it is quick and non-invasive and responds well to millennial-scale variability.

Mathematical discussion

The results of this study clearly illustrate the necessity for broader band discussion of these proxies. While this research suggests perhaps one instance of a significant narrow band oscillation, the general conclusion is that line frequencies are not part of the common makeup of the climate signal. The spectral estimates of reflectance over a 950-kyr interval (Figure 2.0) clearly indicate the pitfalls that may arise from under-smoothing our spectra. While the overall estimations generated by using different numbers of Slepian tapers does not appear to be vastly different, there is enough difference between them (both in the frequency and confidence domains) to warrant caution in our interpretation. Since we may generally assume that climate variability will have appreciable modulation in the frequency and amplitude domains, a broader band smoothing will be absolutely necessary in order to see this.

The use of multiple methods provides greater overall assurance in our statistics. Clearly, the χ^2 confidence intervals should be employed, as they are the 'tried and true' method of spectral analysis. Furthermore, the use of the noise background estimate provides both an opportunity to see how well it 'stacks' up against the standard confidence tests as well as provides a counterpoint to the classic confidence interval. The research here suggests that the noise background estimate (NBE) method is a reasonable method for confidence testing, etc. in the frequency domain but that it must be compared with more traditional methods of confidence testing.

It should again be pointed out that the hypothesis proposed by Mann and Lees that an AR(1) model be fit to the time series is a flawed assumption that greatly oversimplifies the underlying statistics of the climate signal. The findings of this paper,

although not formally documented, were that higher order autoregressive models provided a better fit to the data studied. This was ascertained using Akaike's Information Criterion, which typically gave order 4 or 5 AR fits for densely sampled proxies (GRAPE and magnetic susceptibility) and order 1 or 2 AR fits for less densely sampled ones (Reflectance and natural gamma). This would imply that the characteristic autocorrelation of these proxies is on the order of 1 to 2 kyr over the entire frequency band. This fact might be due to the characteristic ocean overturning rate, which is thought to be ~1000 years. Future research may find the use of AIC or other AR order hypothesis tests informative in understanding the autocorrelation of the climate signal. In point of fact, AR models may also be fit to specific frequency bands in an attempt to better understand the autocorrelation over that regime. This may further assist researcher in understanding the underlying physics governing climate variations. Analysis of the AR coefficients would also assist in this type of research but the intuition behind these coefficients is typically much more difficult to arrive at.

As this research was conducted, it became clear that the length of the time interval used to derive a spectral estimate affects the nature of the spectrum. If a particular climate oscillation (one due to some first-order physical process) displays modulations in either frequency or amplitude, a large time interval may not display a significant central frequency. The use of shorter time intervals then would help us in assessing a characteristic timescale at which the degree of modulation is small enough to derive a significant spectral estimate. An analogy would be the transition between the 100-kyr and the 41-kyr dominated climate approximately 800 to 950 Ka (the Mid-Pleistocene Revolution). If one uses a 1 million year time interval, one would see a very prominent 100-kyr peak and a moderately powerful 41-kyr one. However, if one were to analyze the climate signal over the 1.0 – 1.2 Ka interval, one would find a powerful 41-kyr peak and only a weak 100-kyr peak. Thus, the time interval can be quite useful in zeroing in on characteristic timescales for some oscillations. Spectral evolution may also be used to derive these timescales.

Filtration in the narrow and broad bands should be conducted in the future to test the theory that there may be a phase relationship between GRAPE and magnetic

susceptibility at Site 983. In general, this practice should be carried out anytime there is suspicion of these types of phase relationships.

Again, aliasing should receive at least our consideration. Although we cannot test any aliasing hypothesis from the methods used in this paper, it is a very real concern if we are asserting that a frequency band is statistically significant. Any extreme high-frequency oscillations that may exist in the climate signal recorded by deep-sea sediments may be aliased as a result of undersampling. This will result in a concentration of power at lower frequencies than the aliased frequency. This may lead to the erroneous assumption that lower frequencies represent a real oscillation in the climate signal, when they should be interpreted as an aliased signal.

Conclusion

The results of this paper do not fully answer all the questions posed. They do not provide a great deal of information about age-model concerns or complex sedimentation profiles. However, there is a considerable body of evidence to answer the sub-orbital/millennial-scale line frequency question. The most powerful results come from the proxy and mathematics quarters. Below is a brief list summarizing the results of this study.

1. The method used in this paper was designed to derive potentially significant narrow band oscillations in the climate signal. To fully assess these types of oscillations, coherence plots were also generated in order to crosscheck between proxies. The results indicate that there is no appreciable instance of sinusoidal-type oscillations in the climate signal. The only exception appears to be at Site 983 between the GRAPE and magnetic susceptibility data sets, where there appears to be a coherent period band between ~1.6 – 3.3 kyr. That Site 980 does not display coherence in this period band suggests that we may be witnessing a narrow band oscillation in the ISOW current strength. This variable current may entrain different ratios of biogenic carbonate to terrigenous materials that may be reflected in these two proxies. Future studies should attempt to reproduce these results and employ bandpass filtration methods to assess any phase relationship that may exist between these two proxies.

2. The Heinrich regime, while not displaying any narrow band frequencies, does display a considerable concentration of power between 8.8 and 11.0 kyr. Broad band analysis must be conducted on these proxies to verify this. The binge/purge (Alley and MacAyeal, 1994) and bundling (Bond and Lotti, 1995) hypotheses cannot be tested by the methods used in this paper. Furthermore, the harmonic hypothesis (e.g. Ortiz et al., 1999) cannot be rigorously tested. More work must be conducted to determine if any of these hypotheses can be validated by these proxies.
3. Age-model issues could only be resolved if there was a high degree of coherence and matching spectral peaks within particular narrow frequency bands. This study found only one such instance (discussed above), which does not seem sufficient to make the claim that the age-models are sufficiently resolved. In fact, it is possible (although it seems improbable) that the age-model at Site 983 is adequately resolved while the one at 980 is not. Thus, the results are inconclusive.
4. In consideration of the potential age-model difficulties, which unfortunately cannot be quantified, it is my hope that the orbital timescale can be improved, perhaps by using one or more of the proxies used in this paper. A great deal more work must be conducted at millennial-scale resolution to begin to piece together an overall picture of the Quaternary climate. Once this work is completed, a more thorough timescale may be constructed that will allow confident construction of age-models that have accurate resolution to the millennial level.
5. At the outset of this paper, it was believed that the use of several different proxies at two separate locations in the North Atlantic would provide enough information to help 'tease apart' the 4-component sediment profile at Site 983. However, the results of this analysis did not vary widely enough across proxies to warrant such isolation. Furthermore, identification of independent inputs would theoretically rely upon our ability to isolate narrow band frequencies (as this is the method employed in this paper). Since there was no appreciable instance of coherent narrow band variability, we cannot make any concrete conclusions by this method. The only arguable instance would again be the 1.6 to 3.3 kyr regime found at Site 983, which may be indicative of a variable ocean current strength. It generally appeared that Site 980 proxies showed greater response to sub-orbital variability. This suggests that the stochastic

element at Site 983 was generally higher, which we would certainly expect in the presence of current transport of sedimentary material.

6. GRAPE and magnetic susceptibility proved to be the most robust proxies used in this paper. The degree of resolution and their overall sensitivity made them excellent proxies for the study of sub-orbital climate variability. Natural gamma appears to be extremely sensitive to Milankovitch periodicities and should be used in site-specific age-model construction in the future. Spectral reflectance also proved to be quite robust but the resolution desired was lacking. This brings up the point that time-consuming data retrieval methods will be disfavored aboard sea-going vessels, as there is so much other work to be done. Thus, magnetic susceptibility is clearly one of the best all-around proxies for continued, high-resolution study of pelagic sediments.
7. Broader band analyses must be conducted on all the proxies at both sites. The findings of this paper inform the narrow band discussion but much work remains to be done within the broad band. Of particular interest will be the Heinrich regime between 9 and 11 kyr, which seems to show some concentration of variance within these spectral estimates. Also, a broad band discussion of the potential millennial-scale oscillations found at Site 983 would help to validate the findings here.
8. Future research conducted at these two sites should address filtration issues. Many instances arise where we may wish to analyze a specific frequency range within these data sets in an attempt to derive phase relationships (especially at sub-orbital pacing). The derivation of phase relationships between different proxies and sites may elucidate the 'finer structure' of climate change and how these proxies respond to independent inputs.
9. It became apparent as this study was conducted that the length of the age interval studied bears upon the periodicities derived. The use of spectral methods may assist in determining the time-scale at which sub-orbital oscillations may be thought of as locally non-modulating. Spectral evolution and filtration methods should be employed to determine these time-scales. This may prove invaluable in the discussion of the Heinrich regime between 8.8 – 11.0 kyr as this appears to be a moderately wide, significant band. There are no narrow band frequencies within this

regime so the next step must be to look at the broad band spectrum at a variety of time intervals and evolutively in an attempt to qualitatively describe this regime.

10. The use of AIC (Akaike's Information Criterion) and other more complex model AR (MA or ARMA as well) fitting tests provides insight into the autocorrelation of the climate signal over time. This study finds that these proxies are autocorrelated on a scale from 1 to 2 kyr over the entire frequency band. This may be indicative of the characteristic ocean overturning rate, which is estimated to be ~1000 years. Furthermore, model fitting can be conducted over specific frequency bands to determine the autocorrelation found within these regimes. Thus, it may be possible to show that the DO regime is essentially a white noise process (for example) over some interval, which helps in our understanding of any underlying physical mechanisms. Also, we may consider the coefficients of our AR estimates to derive any underlying principles governing significant oscillations in ancient climate. It should be pointed out that the intuition behind this type of method is much harder to arrive at. Nonetheless, it may prove quite useful if implemented properly.

Appendix

A Brief Explanation of Thomson's Multitaper Method

Conventional Fourier analysis generates the spectral density function by

$$S(f) = \lim_{T\to\infty}[E\{\frac{|F_T(f)|^2}{2T}\}]$$

where

$$F_T(f) = \frac{1}{\sqrt{2\pi}}\int_{-T}^{T} X(t)e^{-2\pi ift}dt$$

is the standard Fourier Transform of the data, *X(t)*. Then the expected value in the first equation gives the average of the energy contributed by *X(t)* at each frequency (Priestley, 1996). Of course, when dealing with discrete time series, we cannot take $T \to \infty$ since we have neither a continuous sample nor an infinite data set. Various methods exist to address this problem, which can be found in Priestley (1996) or other similar texts. Thomson's Method is a modification of the standard spectral density function, where it is desired that a 'tapering' be applied to the function so that we can get a locally more accurate estimate of the spectrum. An orthogonal set of vectors, called Slepian tapers, can be introduced into the Fourier Transform. These vectors are actually eigenvectors and have associated with them, a set of eigenvalues that, by convention, are ordered from 1 to K in decreasing value. The modified Fourier Transform is

$$F_k(f) = \sum_{n=1}^{N} Q_n^{(k)} X_n e^{2\pi ifn\Delta t}$$

(in the discrete form) where $n = 1,\ldots,N$ are the number of samples in the data record, k is the number of tapers to be used, and $Q_n^{(k)}$ (which is necessarily of length N) is the *kth* member of the eigenvector set (Slepian tapers). Then the new estimate of the spectral density is

$$S(f) = \frac{\sum_{k=1}^{K}\lambda_k|F_k(f)|^2}{\sum_{k=1}^{K}\lambda_k}$$

where λ_k is the *kth* eigenvalue associated with the *kth* member of the set of eigenvectors (Mann and Lees, 1996), (Yiou et al,1991).

A few words on this method are necessary. It is not necessary that *S(f)* be eigenvalue-weighted when computing the average. In many instances, it appears that a simple, non-weighted average will suffice. On the other hand, there are very elaborate methods for computing the average (Thomson, 1982). It seemed sufficient for this study, to use the eigenvalue-weighting method. Furthermore, the choice of K, the desired number of tapers, has an appreciable effect upon the spectral estimate. Using fewer tapers allows one to better separate signals that are close together but at the cost of making the overall spectrum more 'jagged' and statistically unstable. There are also tests for determining what number of tapers are best suited to a particular data set (Mann and Lees, 1996).

The F-test

As previously noted, the F-test used in this study was designed to iteratively test the hypothesis that a particular frequency in the spectral estimate explained an abnormally large amount of the variance when compared to the variance explained by a pure sinusoid at that frequency. Given

$$\tilde{F}_k(f) = \sum_{n=1}^{N} Q_n^{(k)} e^{2\pi i f n \Delta t}$$

$$\tilde{F}_{0k} = \tilde{F}_k(0)$$

the Fourier transform of the set of eigenvalues at $f = 0$. And given

$$\mu(f) = \frac{\sum_{k=1}^{K} \tilde{F}_{0k} F_k(f)}{\sum_{k=1}^{K} (\tilde{F}_{0k})^2}$$

a comparative ratio, we then have a form for the F-test

$$T(f) = W(f)\frac{(K-1)|\mu(f)|^2 \sum_{k=1}^{K} (\bar{F}_{0k})^2}{\sum_{k=1}^{K} \left| F_k(f) - \mu(f)\bar{F}_{0k} \right|^2}$$

where *W(f)* is a linear weighting function such that.

$$W(0) = 10$$
$$W(f_{\max}) = 1$$

Again, it should be pointed out that *W(f)* is a modification that is not seen in standard F-tests. The reason for its implementation is because we know ahead of time which frequencies we wish to look at and can therefore tailor the F-test to suit our own needs. A more thorough treatment of this material can be found in Percival and Walden (1993) or Mann and Lees (1996).

Variance Adjustment

As previously mentioned, the total energy of the reshaped spectrum is reduced relative to the original when particular frequencies that passed the F-Test are reduced (power-wise). Since this can have appreciable effects upon our estimate of the spectral power of the background noise, we need to 'shift' the reshaped spectrum back to its original power regime. This was accomplished by assuming that a scalar multiple of the reshaped signal, *N(t)*, would suffice to appropriately 'shift' the spectrum of *N(t)* back to that of *X(t)*. In other words, we start from the assumption that for appropriate *m*

$$S(X(t)) \cong S(mN(t))$$

where *S(X(t))*, *S(N(t))* are defined as the MTM estimates of *X(t)* and *N(t)*. In discrete form, this is equivalent to

$$\sum_{n=0}^{N-1}\sum_{k=1}^{K} \frac{\lambda_k \left| F_k(X(t)) \right|^2}{\sum_{k=1}^{K} \lambda_k} \cong \sum_{n=0}^{N-1}\sum_{k=1}^{K} \frac{\lambda_k \left| F_k(mN(t)) \right|^2}{\sum_{k=1}^{K} \lambda_k}$$

which can be reduced to

$$\sum_{n=0}^{N-1}\sum_{k=1}^{K}\left|F_k(X(t))\right|^2 \cong m^2\sum_{n=0}^{N-1}\sum_{k=1}^{K}\left|F_k(N(t))\right|^2$$
$$N\overline{F}_X \cong m^2 N\overline{F}_N$$

where

$$\overline{F}_X = E[\sum_{k=1}^{K}\left|F_k(X(t))\right|^2]$$
$$\overline{F}_N = E[\sum_{k=1}^{K}\left|F_k(N(t))\right|^2]$$

are the expected values of the absolute squares of the MTM Fourier transforms of both *X(t)* and *N(t)*. Note that taking

$$\overline{F}_X = E[\left|F(X(t))\right|^2]$$
$$\overline{F}_N = E[\left|F(N(t))\right|^2]$$

with *F(X(t))* and *F(N(t))*, the standard Fourier transforms of *X(t)* and *N(t)* will also work. Then

$$m = +\sqrt{\frac{\overline{F}_X}{\overline{F}_N}}$$

the ratio of powers between *F(X(t))* and *F(N(t))*, is the appropriate scalar multiple to make the MTM spectral estimate of *N(t)* as near in total energy to that of *X(t)*.

Coherency

Coherency can be thought of as the 'correlation' between an input and an output, as a function of frequency. In paleoclimatological research, this may be the 'correlation' between theoretical prediction and empirical observation such as has been carried out in testing the Milankovitch hypothesis (Hayes et al., 1976). It may also be used to derive

spatial or temporal relationships between inputs and outputs at single or multiple locations, e.g. Therefore, coherence can be an excellent method for isolating signals that derive from independent inputs.

The basic idea is very simple. If we observe that the *auto*-spectral density can be represented by using the autocovariance, $R_x(\tau)$, of the data set $X(t)$, given by:

$$h(\omega) = \int_{-\infty}^{\infty} R_x(\tau) e^{-i\omega t} d\tau$$

where ω is the period (Priestley, 1996), then we can make an estimate of the spectral density by using the *sample* autocovariance:

$$\tilde{h}(\omega) = \int_{-\infty}^{\infty} \tilde{R}_x(\tau) e^{-i\omega t} d\tau$$

Of course, in practice, this method has distinct limitations since the sample autocovariance for discrete, finite time-series becomes more statistically inaccurate (unstable) for τ large.

Then, we may define the cross-spectral density function by:

$$h_{xy}(\omega) = \int_{-\infty}^{\infty} R_{xy}(\tau) e^{-i\omega t} d\tau$$

where $R_{xy}(\tau)$ is defined as the cross-covariance between $X(t)$ and $Y(t)$. Thus, we may proceed just as we did above by observing that an estimate of the cross-spectral density can also be defined by the sample cross-covariance:

$$\tilde{h}_{xy}(\omega) = \int_{-\infty}^{\infty} \tilde{R}_{xy}(\tau) e^{-i\omega t} d\tau$$

Another method for deriving the cross-spectral density function is to use the convolution of $X(t)$ and $Y(t)$:

$$\tilde{h}_{xy}(\omega) = E[\int_{-\infty}^{\infty} X(t) * Y(t) e^{-i\omega t} d\tau]$$

The drawback of using the cross-spectral density function is that it is not normalized so that we do not know how 'strong' the correlation is between *X(t)* and *Y(t)* unless both data sets are very simple. This is almost always the effect when dealing with real paleoclimate data sets. To deal with this, we introduce the coherency function, which is defined as:

$$\left|\tilde{W}_{xy}(\omega)\right| = \frac{\left|\tilde{h}_{xy}(\omega)\right|}{\left\{\tilde{h}_x(\omega)\tilde{h}_y(\omega)\right\}^{1/2}}$$

which is bounded by $1 \geq mag(W_{xy}(\omega)) \geq 0$. Thus, the coherency function can be utilized to estimate the 'correlation' between *X(t)* and *Y(t)* by telling us how much the variance due to a particular frequency or period in *X(t)* is 'correlated' to that period or frequency in *Y(t)*. 95% confidence intervals for non-zero coherence are also necessary.

The reader is referred to Priestley (1996), Bendat and Piersol (1986), or other similar materials for a more thorough treatment of methods and applications of coherence functions

Akaike's Information Criterion (AIC)

The AIC is one of many methods used to determine what order AR (or ARMA) model best fits a data set. The basic procedure is to make parameter estimations under a number of order hypotheses and see which one best fits the data. In other words, we estimate the parameters of an AR(k) process for k = 1,...,n where we arbitrarily choose some upper limit, n, beyond which we assume higher order autoregressive models could not provide a better estimate. Next, we test these parameters to see how well they explain the statistical structure of the data. The crux of the test is concerned with the variance of the residual, which, as the order of the model approaches a best fit, goes to white noise.

Recall that the form of an AR(k) process is.

$$x(t) + b_1 x(t-1) + b_2 x(t-2) + ... + b_k x(t-k) = \varepsilon_t$$

Where b_j are the autoregressive coefficients and ε_t is a white-noise process. It is known that AIC reduces to

$$AIC(k) = n\log_{10}(FPE(k))$$

$$FPE(k) = \frac{n+k}{n-k}\sigma_{\varepsilon}^{'2}$$

where *FPE(k)* is known as the final prediction error given by

$$\sigma_{\varepsilon}^{'2} = \{R'(0) + b_1'R'(1) + ... + b_k'R'(k)\}$$

$R'(\tau)$ is the autocorrelation of the AR(k) estimate and b_j' are the coefficients of this estimate. When the graph of *AIC(k)* flattens out or reaches a distinct minimum, the order

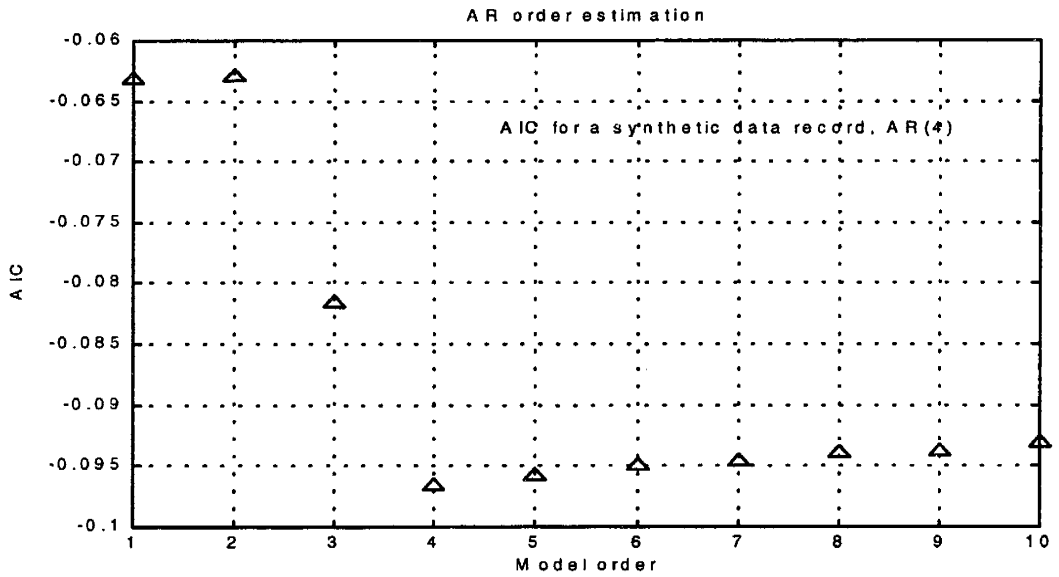

Figure A1.1. Display of the Akaike's Information Criterion test for AR order determination. A synthetic data set of 1000 points was created with 4 random autoregressive coefficients.

of the AR process that best fits the data has been found (Priestley, 1996). We can further simplify the *AIC(k)* by realizing that n is simply a multiplicative constant. Thus, Akaike's Information Criterion states that

$$\min(AIC(k)) = \min(\log_{10}(FPE(k))$$

gives us an estimate of the order autoregressive model that best fits a given data set.

Singular Spectral Filtration

Singular spectral analysis is a newer method of time series analysis that hinges upon simple linear algebraic concepts. Its simplicity and elegance make it a very powerful method, which will undoubtedly see widespread use in the future. The basic idea is very simple. If you have a time series *X(t)* that is uniformly sampled, demeaned, and detrended, you start be creating its trajectory matrix:

$$\mathbf{L} = \begin{bmatrix} x(1) & x(2) & x(3) & . & . & x(k) \\ x(2) & x(3) & x(4) & . & . & x(k+1) \\ x(3) & x(4) & x(5) & . & . & x(k+2) \\ . & & & . & & \\ . & & & & . & \\ x(n-k+1) & . & . & . & . & x(n) \end{bmatrix}$$

where n is the length of the record *X(t)*. k is known as the window length and it plays an important role in isolating periodic signals. Since each row in **L** has length k, we are essentially subdividing *X(t)* into $n-k+1$ 'sub-realizations' and **L** becomes a sample ensemble record of $n-k+1$ realizations each of length k. The choice of k then determines what frequencies we can reasonably study. Since k functions as a moving window over the *X(t)*, periodicities with wavelengths $k\Delta t$ are the lowest periods that can be resolved. The reader might infer that taking large k then would be the best course of action. However, Elsner and Tsonis (1995) suggest that $k = n/4$ is the optimal window length. This is the window length that has been used in this paper.

Next, we take:

$$\mathbf{R} = \mathbf{L}^T\mathbf{L}$$

R is called the lagged-covariance matrix. The reason for this should be obvious when we consider that $\mathbf{L}^T\mathbf{L}$ is a square symmetric matrix whose entries correspond to the truncated

variances and covariances of $X(t)$, up to a normalization. The crux of SSA is in observing that, in most cases, **R** has a spectral decomposition given by:

$$\mathbf{R} = \mathbf{Q}\Lambda\mathbf{Q}^T$$

Where **Q** is the matrix of eigenvectors of **R** and Λ is the diagonal matrix of eigenvalues. By convention $\boldsymbol{q}_i$ is associated with λ_i where $1 \leq i \leq k$ and λ_1. λ_2, ..., λ_k are arranged in descending order.

Since eigenvectors are orthogonal, **Q** actually represents a basis for the lagged-covariance matrix **R**. Thus, we may create projections by:

$$\mathbf{R}' = \mathbf{R}\mathbf{Q}_m\mathbf{Q}_m^T$$

where $\mathbf{Q}_m$ is some submatrix of **Q**. Keep in mind that all the $\boldsymbol{q}_i$ are orthogonal.

Some word should be made about the physical intuition behind the matrices containing the eignevectors/values. When dealing with time series or other data sets that are believed to contain periodic oscillations, the spectral decomposition of the lagged-covariance matrix has the effect of organizing oscillations according to their relative contribution to the overall variance of the signal. Thus, if the 19 kyr periodicity were responsible for half the overall variance in a time series, the highest (in the value sense) eigenvectors/values (i.e. $\boldsymbol{q}_1$, $\boldsymbol{q}_2$ and λ_1. λ_2) would 'record' this oscillation. In this regard, SSA is somewhat more difficult to work with than Fourier analysis since the power spectral density is readily interpreted as power concentrated at a particular frequency. SSA does not make this distinction (at least not in graphical form) so that the highest eigenvalues (roughly equivalent to the most powerful concentration of energy in a power density spectrum) do not necessarily correspond with the lowest frequencies – under the assumption that we are considering non-white noise processes. However, since the nature of the power spectrum density associated with climate variability is generally one of decreasing power with frequency, it is often fair to assume that the first several pairs of eigenvectors/values will be associated with the low-frequency component of the record.

One last word should be made concerning time series reconstruction. It has been found that eigenvectors should be taken in pairs for time series reconstruction (Elsner

Tsonis, 1995). The exact reasons for this have not yet been clarified but it could be that eigenvectors behave similarly to sine and cosine functions (indeed they are both orthogonal constructs) in that Fourier analysis frequently requires sine/cosine pairs to represent a data set.

Time series reconstruction is conducted in a two-step process as follows:

$$a_i^m = \sum_{j=1}^{k} x(i+j-1)q_j^m$$

$$\tilde{x}(i+j-1) = \sum_{m=1}^{k} a_j^m q_j^m$$

for $i = 1, 2, \ldots, n, j = 1, 2, \ldots, k$ where q_j^m is the jth component of the mth eigenvector. This is just the numerical convolution of the principal components with the corresponding eigenvectors (Tsonis and Elsner, 1995). A more succinct way of expressing the above is:

$$\tilde{\mathbf{L}} = \mathbf{L}\mathbf{Q}_m\mathbf{Q}_m^T$$

which states that the reconstructed trajectory matrix is merely the projection of **L** onto some subspace denoted by $\mathbf{Q}_m$. Thus, we can easily extract the reconstructed time series by noticing that **L** contains the complete ordered set of *X(t)* along its first column concatenated with its last row (less the common element $L_{n-k+1,1}$).

Filtration via SSA amounts to choosing $\mathbf{Q}_m$ so that you reconstruct a time-series that excludes certain periodicities according to their contribution to the overall variance. This information can be inferred from the eigenvalues since they are ordered according to the amount of variance their corresponding periodicities contribute to the overall variance of *X(t)*. Thus, in constructing a 'high-pass' filter for climate variability we would choose $\mathbf{Q}_m$ so that it excluded the first several eigenvector pairs associated with a greater portion of the overall variance. This method is somewhat imperfect since it is still necessary to compare the estimated power spectral density functions of *X(t)* and *X'(t)* to verify that the proper frequencies have been filtered. Nonetheless, SSA filtration provides a quick and reliable method for filtering out whichever frequencies one desires.

References

1. Alley, R.B., MacAyeal, D.R., Ice-rafted debris associated with binge/purge oscillations of the Laurentide Ice Sheet. *Paleoceanography*, **Vol. 9, No. 4**, 503-511 (1994)
2. Bendat, J.S., Piersol, A.G., 1986 *Random Data: Analysis and Measurement Procedures.* John Wiley & Sons, Inc.
3. Bond, G, et al., Correlations between climate records from North Atlantic sediments and Greenland ice. *Nature* **365**,143-147 (1993)
4. Bond, G., *et al.* A pervasive millennial-scale cycle in North Atlantic Holocene and glacial times. *Science* **278**, 1257-1266 (1997).
5. Bond, G., Lotti, R., Iceberg discharges into the North Atlantic on millennial timescales during the last glaciation. *Science* **267**, 1005-1010 (1995)
6. Boyce, R.E, et al., DSDP Leg 33 procedure using the gamma ray attenuation porosity evaluator (GRAPE). *Initial Reports of the Deep Sea Drilling Project, Scientific Results*, **Vol. 33**, 935 –951 (1976)
7. Broecker, W., et al., Origin of the North Atlantic's Heinrich events. *Climate Dynamics* **6**, 265-273 (1992)
8. Carter, S., Raymo, M.E., Sedimentological and mineralogical control of multi-sensor-track data at Sites 981 and 984. Submitted for publication September 1, 1997
9. Cortijo, E., et al., Sedimentary record of rapid climate variability in the North Atlantic during the last glacial cycle. *Paleoceanography*, **Vol. 10, No. 5**, 911-926 (1995)
10. Crowley, C.J., North, G.R., 1991 *Paleoclimatology*, Oxford Press, Inc., NY pp.132-145
11. Dansgaard, W., et al., Evidence for general instability of past climate from a 250-kyr ice-core record. *Nature* **364**, 218-222 (1993)
12. Elsner, J.B., Tsonis, A.A., 1996 *Singular Spectral Analysis*, Plenum Press, NY
13. Hartmann, D.L, 1994 *Global Physical Climatology*, Academic Press, NY pp. 110-112, 210, 302-312
14. Hays, J.D., Imbrie, J., Shackleton, N.J., Variations in the earth's orbit: Pacemaker of the ice ages. *Science* **194**, 1121-1132 (1976)
15. Heinrich, H., Origin and consequences of cyclic ice rafting in the Northeast Atlantic during the past 130,000 years. *Quaternary Research* **29**, 142-152 (1988)
16. Hoppie, B.W., Blum, P., and Shipboard Scientific Party, Natural gamma measurements on ODP cores: Introduction to procedures with examples from Leg 150. *The Proceedings of the ODP, Initial Reports*, **Vol. 150**, 51-59 (1994)
17. Imbrie, J., et al., The theory of Pleistocene climate: Support from a revised chronology of the marine $\delta^{18}O$ record. *Milankovitch and Climate* **Vol.1**, edited by A. Berger et al., pp. 269-305, Norwell, MA, 1984
18. Jansen, E., et al., Evolution of Pliocene climate cyclicity at Hole 806B (5-2 Ma): Oxygen isotope record. *Proceedings of the ODP, Scientific Results*, Vol. **130**, 349-362 (1993)
19. Jansen, E., Raymo, M.E., Blum, P., Shipboard scientific party, Leg 162: New frontiers on past climate. *The Proceedings of the ODP, Initial Reports*, Vol. **162,** 5-209 (1995)

20. Keigwin, K.D., Jones, G.A., Western North Atlantic evidence for millennial-scale changes in ocean circulation and climate. *Journal of Geo. Res.* **99**, 12,397-12,410 (1994)
21. MacAyeal, D.R., A low-order model of the Heinrich event cycle. *Paleoceanography*, **Vol. 8, No. 6**, 767-773 (1993)
22. MacAyeal, D.R., Binge/purge oscillations of the Laurentide Ice Sheet as a cause of the North Atlantic Heinrich events. *Paleoceanography*, **Vol. 8, No. 6**, 775-784 (1993)
23. Mann, M.E, Lees, J.M, Robust estimation of background noise and signal detection in climatic time series. *Climate Change* **33**, 409-445 (1996)
24. Marotzke, J., Willebrand, J., Multiple equilibria of the global thermohaline circulation. *Journal of Physical Oceanography*, **Vol. 21**, 1372-1385 (1991)
25. Oppo, D.W., McManus, J.F., Cullen, J.L. Abrupt climate events 500,000 to 340,000 years ago: Evidence from subpolar North Atlantic sediments. *Science* **279**, 1335-1339 (1998)
26. Ortiz, J., Mix, A., Harris, S., O'Connell, S., Diffuse spectral reflectance as a proxy for percent carbonate content in North Atlantic sediments. *Paleoceanography* **Vol.14, No. 2**, 171-185 (1999)
27. Percival and Walden
28. Percival, D.B., Walden, A.T., 1993 *Spectral Analysis for Physical Applications.* Cambridge University Press, pp. 331-374
29. Priestley, M.B, Probability and mathematical statistics: Spectral analysis and time series. Academic Press, Boston, pp. 346-354, pp. 378-380, 1996
30. Raymo, M.E, et al., Millennial-scale climate instability during the early Pleistocene epoch. *Nature* **392**, 699-702 (1998)
31. Raymo, M.E., et al, Millennial-scale climate instability during the early Pleistocene epoch. *Nature* **392**, 699-702 (1998)
32. Raymo, M.E., The timing of major climate terminations. *Paleoceanography* **Vol. 12, No. 4**, 577-585 (1997)
33. Robinson, S.G., Lithostratigraphic applications for magnetic susceptibility logging of deep-sea sediment cores: Examples from ODP Leg 115. In E.A Hailwood and R.B Kidd, *editors*, *High Resolution Stratigraphy*, pp. 65-98. The Royal Society, London, 1993
33. Ruddiman, W.F., Marine indicators of Wisconsonian Laurentide ice volume. *Congress of the International Union for Quaternary Research*, **Vol. 12**, p.256 (1987)
35. Shackleton, N.J., Berger, A., Peltier, W.A., An alternative astronomical calibration of the lower Pleistocene timescale based on ODP Site 677. *Transactions of the Royal Society of Edinburg: Earth Sciences*, **Vol. 81, No. 4**, 251-261 (1990)
36. Thomson, D.J., Spectrum estimation and harmonic analysis. *Proc. IEEE* **70**, 1055-1096 (1982)
37. Yang, Q., et al., Major features of glaciochemistry over the last 110,000 years in the Greenland Ice Sheet Project 2 ice core. *Journal of Geophysical Research*, **Vol. 102, No. D19**, 23,289-23,299 (1997)
38. Yiou, et al., High-frequency paleovariability in climate and CO_2 levels from Vostok ice core records. *Journal of Geophysical Research, B, Solid Earth and Planets*, **Vol. 96, No. 12**, 20,365-20,378 (1991)

THESIS PROCESSING SLIP

FIXED FIELD: ill. _____ name _____

index _____ biblio _____

▶ COPIES: (Archives) Aero Dewey Eng Hum

(Lindgren) Music Rotch Science

TITLE VARIES: ▶☐ _____

NAME VARIES: ▶☐ _____

IMPRINT: (COPYRIGHT) _____

▶ COLLATION: 73 P

(pages with graphs are unnumbered)

▶ ADD: DEGREE: _____ ▶ DEPT.: _____

SUPERVISORS: _____

NOTES:

cat'r: date:

page: F62

▶ DEPT: EAPS

▶ YEAR: 2000 ▶ DEGREE: S.M.

▶ NAME: COLES, Darrell Ardon